Czech Technical University in Prague
Faculty of Mechanical Engineering
Department of Energy Engineering

Carbon Capture and Storage

by

Jan Petřík

A bachelor thesis submitted to
the Faculty of Mechanical Engineering, Czech Technical University in Prague,
in partial fulfilment of the requirements for the degree of Bachelor.

Bachelor degree study programme: Theoretical Fundamentals of Mechanical Engineering

Prague, May 2017

Title of the thesis:
Carbon Capture and Storage

Bc. student:
Jan Petřík
Email: jan.petrik@fs.cvut.cz

Supervisor:
doc. Ing. Václav Dostál, Sc.D.
Email: vaclav.dostal@fs.cvut.cz

Address:
Department of Energy Engineering
Faculty of Mechanical Engineering
Czech Technical University in Prague
Thákurova 7
166 29 Prague 6
Czech Republic

Declaration

Author
Jan Petřík

Thesis
Carbon Capture and Storage

I hereby affirm that this bachelor thesis has been written by myself, under the supervision of doc. Ing. Václav Dostál, Sc.D.

All sources of information that have been used in the bachelor thesis are acknowledged in the text and listed in the Bibliography, in accordance with the requirements given by the CTU Guideline.

.....
Jan Petřík
Prague, May 2017

Abstract sheet

Author's name: Jan Petřík
Title of the bachelor thesis: Carbon Capture and Storage
Academic year: 2016/2017
Department/Section: Department of Energy Engineering/ Nuclear Power Engineering Equipment
Supervisor: doc. Ing. Václav Dostál, Sc.D.
Bibliographic data:
Number of pages: 101
Number of pictures: 48
Number of tables: 16
Number of attachments: 2

Abstract:

The aim of the thesis is to explore the issue of carbon capture and energy storage. Essential information about the technology including an overview of existing and planning projects are provided. The functional model designed with an emphasis on self-contained production of components serves as a practical example. This was accomplished using 3D printing, milling and turning. Self-assembled machines were used in most cases. Last but not least, software for compression ratio and efficiency of centrifugal compressor frequently used for energy storage was programmed. Following this, the compressor geometry was slightly modified in order to maximize compression ratio. This was achieved by programmed genetic algorithms with a final increase of almost 30 %.

Keywords:

Carbon capture and storage, accumulation of electrical energy, programming in Python, genetic algorithms, centrifugal compressor, electronics, experiment, 3D printing.

Anotační list

Jméno autora: Jan Petřík
Název bakalářské práce: Zachyt a ukládání uhlíku
Anglický název: Carbon Capture and Storage
Akademický rok: 2016/2017
Ústav/Odbor: Ústav Energetiky/ Jaderná energetická zařízení
Vedoucí BP: doc. Ing. Václav Dostál, Sc.D.
Bibliografické údaje:
Počet stran: 101
Počet obrázků: 48
Počet tabulek: 16
Počet příloh: 2

Anotace:

Cílem bakalářské práce je přiblížit problematiku zachytávání uhlíku a akumulace elektrické energie. Jsou poskytnuty základní informace o této technologii včetně přehledu existujících a plánovaných projektů. Jako praktická ukázka slouží funkční model zkonstruovaný s důrazem na vlastní výrobu komponent. Toho bylo docíleno využitím 3D tisku, frézování a soustružení. Většina operací probíhala na vlastnoručně sestavených strojích. V neposlední řadě byl navržen software pro výpočet kompresního poměru a účinnosti radiálního kompresoru, který se často používá při akumulaci elektrické energie. Geometrie kompresoru byla následně lehce modifikována za účelem zvýšení kompresního poměru. Ten byl zvýšen pomocí naprogramovaného genetického algoritmu téměř o 30 %.

Klíčová slova:

Záchyt a ukládání uhlíku, akumulace elektrické energie, programování v Pythonu, genetické algoritmy, radiální kompresor, elektronika, experiment, 3D tisk.

Acknowledgements

I would like to thank my supervisor doc. Ing. Václav Dostál, Sc.D. for valuable advice and assistance in solving bachelor thesis. Thanks also go to my family for the creation of pleasant background and unfailing support.

Contents

List of Figures

List of Tables

List of Algorithms

Abbreviations

AA-CAES	**A**dvanced **A**diabatic **C**ompressed **A**ir **E**nergy **S**torage
A-CAES	**A**diabatic **C**ompressed **A**ir **E**nergy **S**torage
CAES	**C**ompressed **A**ir **E**nergy **S**torage
CAPEX	**Cap**ital **Ex**penditure
CAES	**C**ompressed **A**ir **S**torage
CCC	**C**ryogenic **C**arbon **C**apture
CCS	**C**arbon **C**apture **a**nd **S**torage
CFD	**C**omputational **F**luid **D**ynamics
CNC	**C**omputer **N**umerical **C**ontrol
C-HyPES	**C**losed **H**ydro-**P**neumatic **E**nergy **S**torage
D-CAES	**D**iabatic **C**ompressed **A**ir **E**nergy **S**torage
ECBM	**E**nhanced **C**oal **B**ed **M**ethane **R**ecovery
EEPR	**E**uropean **E**nergy **P**rogramme for **R**ecovery
EGR	**E**nhanced **G**as **R**ecovery
EOR	**E**nhanced **O**il **R**ecovery
FET	**F**ield-**E**ffect **T**ransistor
FPSO	**F**loating **P**roduction **S**torage and **O**ffloading
GCCSI	**G**lobal **C**arbon **C**apture and **S**torage **I**nstitute
GA	**G**enetic **A**lgorithm
GHG	**G**reen**h**ouse **G**as
GUI	**G**raphical **U**ser **I**nterface

HDD	**H**ard **D**isk **D**rive
HP	**H**igh **P**ressure
I-CAES	**I**sothermal **C**ompressed **A**ir **E**nergy **S**torage
IGCC	**I**ntegrated **G**asification **C**ombined **C**ycle
IPCC	**I**ntergovernmental **P**anel on **C**limate **C**hange
LAES	**L**iquid **A**ir **E**nergy **S**torage
LP	**L**ow **P**ressure
LPG	**L**iquefied **P**etroleum **G**as
MCT	**M**ineral **C**arbonation **T**echnology
MOF	**M**etal **O**xide **F**ramework
NGCC	**N**atural **G**as **C**ombined **C**ycle
NGO	**N**on-**G**overnmental **O**rganization
NZEC	**N**ear **Z**ero **E**mission **C**oal
O-HyPES	**O**pen **H**ydro-**P**neumatic **E**nergy **S**torage
OOIP	**O**riginal **O**il **I**n **P**lace
OPEX	**Ope**rating **Ex**pense
pH	**p**otential of **H**ydrogen
PHES	**P**umped **H**eat **E**lectrical **S**torage
PSA	**P**ressure **S**wing **A**dsorption
PWM	**P**ulse **W**idth **M**odulation
RCSP	**R**egional **C**arbon **S**equestration **P**artnerships
RES	**R**enewable **E**nergy **S**ources
RPM	**R**evolution **p**er **M**inute
SW	**S**oft**w**are
TES	**T**hermal **E**nergy **S**torage
US	**U**nited **S**tates
WGS	**W**ater **G**as **S**hift

Symbols

Nomenclature

A	flow area
b^*	ratio of vaneless diffuser inlet width to impeller exit width
c	absolute velocity
C_h	skin friction coefficient
D	diameter
D_f	diffusion factor
I	current
L_f	impeller flow length
$\dot{m}$	mass flowrate
Ma	Mach number
n	revolutions per minute
p	pressure
P	power
Re	Reynolds number
T	temperature
u	tangential velocity
V	voltage
W	work
z	number of blades

α	absolute flow angle
β	relative flow angle
Δh	loss
ϵ	wake fraction of blade-to-blade space
η	efficiency
μ	slip factor
ρ	fluid density
ω	relative velocity

Subscripts

01	overall condition at the impeller inlet
1	impeller inlet
2	impeller exit
a	axial
b	blade
bld	blade loading
h	hub
hyd	hydraulic
i	incidence
inc	incidence
m	meriditional direction
mid	middle
mix	mixing
r	radial
re	recirculation
rel	relative
s	shroud
sf	skin friction
u	peripheral
θ	tangential direction

Chapter 1

Introduction

The primary objective is to acquaint carbon capture and energy storage with the help of technology model and python computation with a genetic algorithm. The bachelor thesis is composed of four thematically different chapters. For this reason, comprehensive explanation of each topic is described within the related chapter.

1.1 General state of the art

Nowadays, environmental impact of operation of power plants is discussed more than ever. Chapter offering answers to the question relating to this topic is called *Carbon Capture a Storage*. As the name suggests, *Energy Storage* chapter which builds on the previous one is dedicated to energy storage problem. Due to studying at the Faculty of Mechanical Engineering, I naturally felt the desire to construct something substantial. Finally, it was decided to construct and build a functional model of energy storage technology. Chapter *Model of Energy Storage Technology* introduces this issue. The last chapter named *Calculations and Optimization via Python* aims to program the software for the calculation of compressor operational values. The compressor was chosen because of the usage in model and for available real input, geometry parameters. However, the geometry of manufactured compressor is different due to the 3D print technology. Genetic algorithm was also developed. The intention was to optimize impeller geometry in order to maximize the compression ratio of the compressor. *Conclusions* chapter summarizes the whole bachelor thesis, offers topics for future work and also reveals my motivation during the research.

1.2 Goals of bachelor thesis

The goals of this thesis are as follows:

- to provide research on the carbon capture and energy storage topic;
- to assemble functional model of air energy storage providing electric energy;
- to calculate isoentropic efficiency, pressure ratio and optimize parameters of centrifugal compressor;

1.3 Structure of bachelor thesis

The thesis is organized into seven chapters as follows:

1. *Introduction*: Provides the general overview of the tackled problems and describes the structure and goals of this bachelor thesis.
2. *Carbon Capture and Storage*: Presents the carbon capture and storage technology. Technological procedures, implemented projects and also economic analysis are mentioned.
3. *Compressed Air Energy Storage*: Describes the energy storage technology using pressurized air called CAES. The basic principles as well as existing power plants are discussed.
4. *Model of Energy Storage Technology*: Introduces functional model of air storage and subsequently, production of electricity.
5. *Calculations and Optimization via Python*: Provides a computational software of centrifugal compressor efficiency and proposes the optimization of the compressor parameters based on genetic algorithm to increase the compression ratio.
6. *Conclusions*: Summarizes the results of the bachelor thesis and suggests possible topics for further research.

Chapter 2

Carbon Capture and Storage

The headline statement from the IPCC report says: „Warming of the climate system is unequivocal, and since the 1950s, many of the observed changes are unprecedented over decades to millennia. The atmosphere and ocean have warmed, the amounts of snow and ice have diminished, sea level has risen, and the concentrations of greenhouse gasses have increased“ (IPCC, 2014). In the event that we take these findings seriously, it is high time to act. One of the possible solutions can be carbon capture and storage technology which is clarified in the following chapter.

2.1 Capture of CO_2

The goal of CO_2 capture is to produce a concentrated stream that can be easily transported. Carbon capture could consume from 25 to 40 % of the fuel energy of a power plant and be responsible for 70 % or more of the additional costs in CCS (Haszeldine, 2009). There exist three main options for capturing CO_2 for industrial and power plants. As shown in Figure 2.1, they are assorted as post-combustion, oxyfuel combustion and precombustion decarbonization (Maroto-Valer, 2010a).

2.1.1 Post-combustion

Post-combustion capture involves separation of CO_2 from the flue gasses produced by combustion of a primary fuel (coal, natural gas, oil or biomass) in air (Maroto-Valer, 2010a). This technology brings advantages such as flexibility in switching between

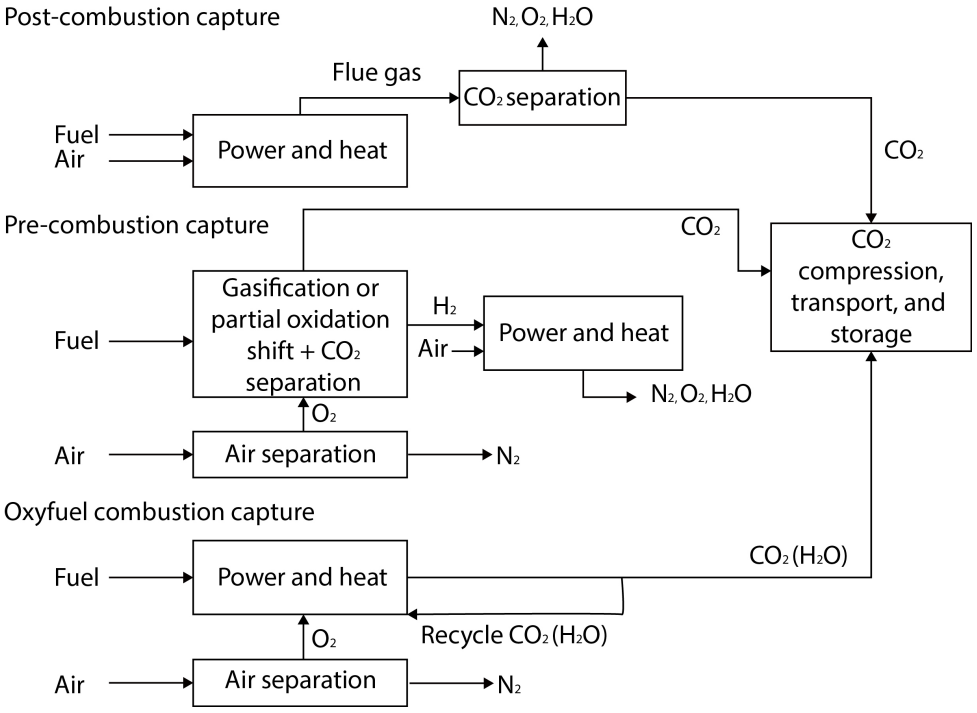

Figure 2.1: Carbon Capture processes (Maroto-Valer, 2010a).

capture/no capture, available solvent technologies, which are proven at pilot scale and an option of retrofit to existing plants. Nevertheless, the equipment would be large in comparison with the footprint size of a coal-fired power plant, great volumes of solvents are required and also consumption of water needs to be reduced. Only Boundary Dam facility in Saskatchewan, Canada using this process is in operation state at the moment. The main challenge to the future is reducing post-combustion retrofitting losses in efficiency (now 10 %) with existing technologies (Al-Fattah et al., 2011; Haszeldine, 2009).

2.1.2 Oxyfuel combustion

Oxyfuel combustion uses pure oxygen instead of air to produce a flue gas that mainly consists of H_2O and CO_2 (Metz et al., 2005). The benefits include easy separation of CO_2 without solvents, smaller physical size and the potential to retrofit on existing plants. On the other hand, high-temperature materials are required and also the issue with ignition and flame stability was found. Currently, two pilot plants using

this process are in operation: Schwarze Pumpe in Germany which is described in Subsection 2.7.4 and Lacq in southwest France (see Monne and Prinet, 2013). Further development focuses on assessment of retrofits for electricity cost, cost of CO_2 avoided (see Subsection 2.6.1) and amelioration of high-temperature operation (Buhre et al., 2005; Haszeldine, 2009).

2.1.3 Pre-combustion

In pre-combustion capture process, coal or fossil fuel undergoes a gasification or reforming stage to produce a syngas which is prepared for extraction of fuel gas and CO_2 due to water-gas shift (WGS) (Maroto-Valer, 2010a). An additional added value of this process is the possibility to switch between hydrogen production and power generation (co-production of hydrogen and power) depending on the power demand. Due to the technology maturity and similarities, pre-combustion CO_2 capture can be applied to high CO_2 emitting industries such as chemical (gas and coal based) and iron & steel. Only Weyburn-Midale Project described in more detail in Subsection 2.7.3 operates with pre-combustion technology at the moment. Finally, it should be noted that high construction costs and decreased short-term flexibility have prevented the development of pre-combustion technology in the last decade at the expense of post-combustion process with improved and new chemical solvents (Haszeldine, 2009; Jansen et al., 2015).

2.2 Separation methods

As shown in Figure 2.2, several separation techniques are used for each capture method. The selection of right technology requires knowledge of the fuel composition, the heat, the influence of water, the resulting partial pressure of the gas mixture and the configuration of the power plant (Rao and Rubin, 2002).

2.2.1 Absorption

Absorption is feasible using two methods. The first technique is called physical absorption which is based on Henry's Law. CO_2 is absorbed under a high pressure

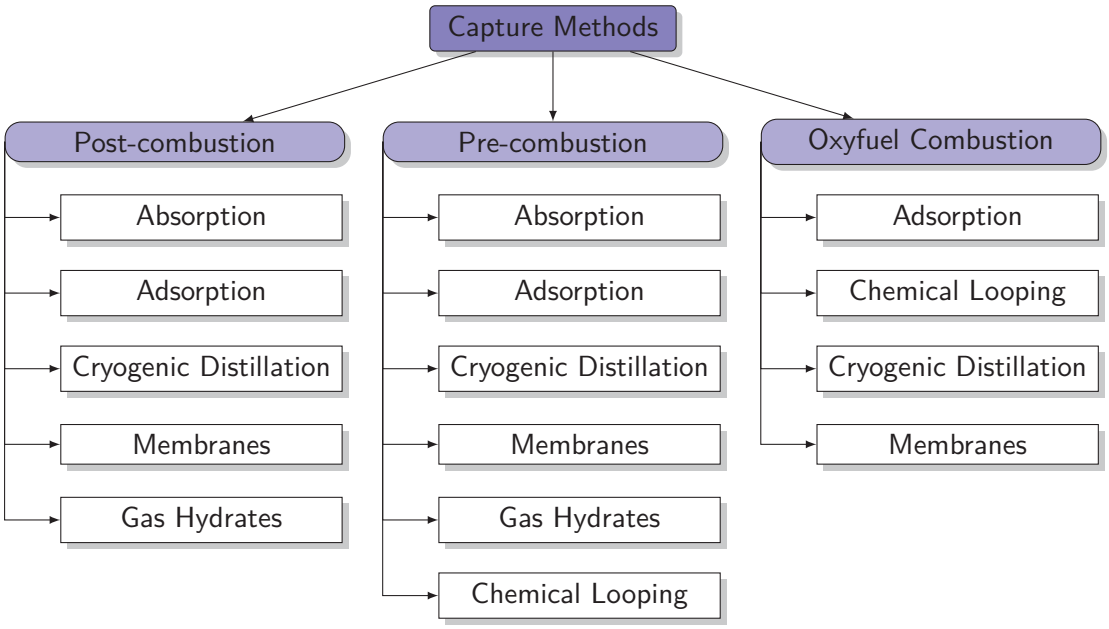

Figure 2.2: Carbon dioxide capture methods possible for each combustion location (D'Alessandro et al., 2010).

and low temperature. After that, it is desorbed at reduced pressure and increased temperature (Cheng-Hsiu, 2012). The second technique is chemical absorption which is depicted in Figure 2.3. The principle is to separate CO_2 from a flue gas using an amine-based solvent process in which CO_2 reacts with a liquid absorbent. The reversibility of chemical reaction leads to the following process stages:

- Absorption process where the solute or component to be absorbed (e.g., CO_2) is transferred from the gas phase to the liquid phase (Wilcox, 2012).
- Stripping process where mass transfer occurs from the liquid to the gas phase (Wilcox, 2012).

On the grounds of huge amount of the flue gasses, there is a need to treat low CO_2 partial pressure in flue gas for post-combustion power plants. Chemical absorption is definitely more suitable than physical absorption to accomplish CO_2 capture purpose. On the other hand, chemical absorption is an energy intensive process in which more than 60 % of total energy is consumed in stripper for thermal regeneration of CO_2 rich chemical absorbents. In the outcome, absorption processes are high efficient

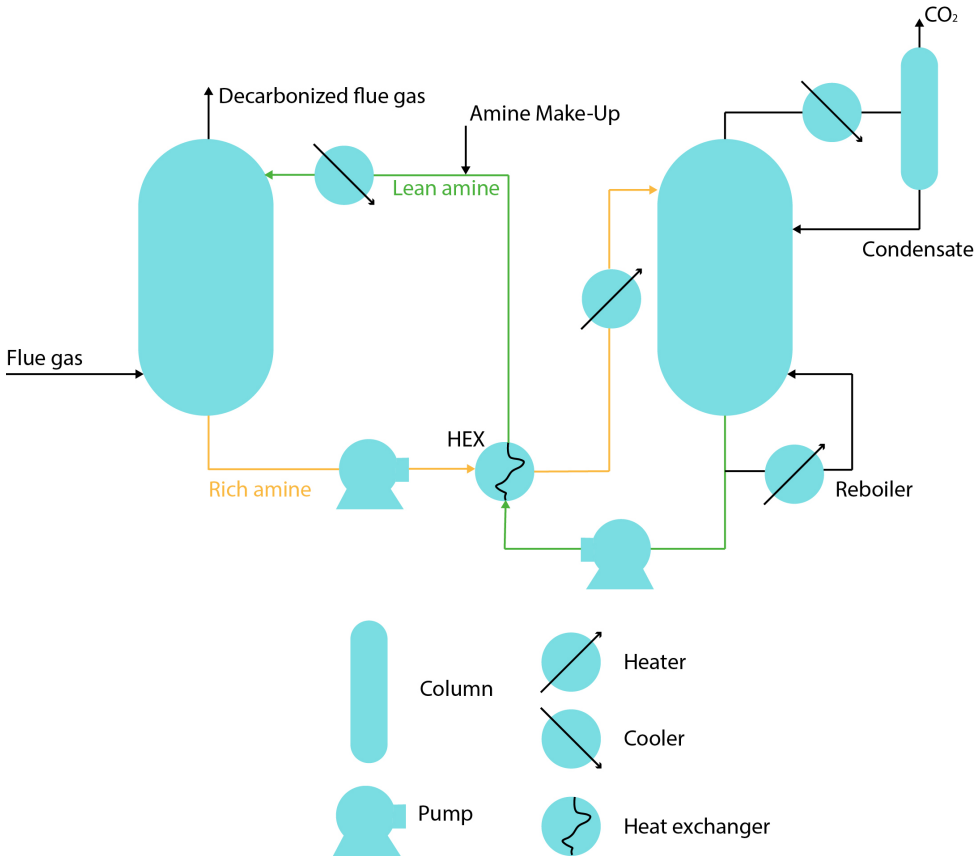

Figure 2.3: Process flow diagram for CO_2 absorption process (Al-Fattah et al., 2011).

systems and lowest costs compared to other post-combustion capture processes. However, there is still a strong need for research and development to decrease operating plant costs, the energy penalty for regeneration and to ameliorate the lifetime of the absorbents (Maroto-Valer, 2010a; Cheng-Hsiu, 2012).

2.2.2 Adsorption

In an adsorption process, a gas mixture contacts small porous particles which can selectively adsorb with CO_2 for its effective removal from the gas mixture (Wilcox, 2012). Common adsorbent frameworks for CO_2 capture include activated carbon and zeolites or capacity metal organic frameworks (MOFs) (see Li et al., 2011). Most applications are associated with pressure swing adsorption (PSA). It is suitable for pure hydrogen applications but with the syngas compositions usually obtained, the hydro-

gen losses would be unacceptable. The development of a new generation of materials that would efficiently adsorb CO_2 will undoubtedly enhance the competitiveness of adsorptive separation in a flue gas application (Metz et al., 2005).

2.2.3 Cryogenic Distillation

The process of cooling a gas mixture to cause a phase change for effective separation is named cryogenic distillation (Wilcox, 2012). The flue gas enters the capture system and is cooled by a series of heat exchangers (only one is shown in Figure 2.4 for simplification) until it reaches the temperature at which the CO_2 freezes to form a nearly pure solid where it is separated easily from the remaining gasses. At this stage of process, two separate streams exist – the pressurized solid CO_2 stream and the CO_2-lean flue gas stream at ambient pressure. Afterwards, the recuperative heat exchangers accomplish warm of both streams. As the solid CO_2 warms, it melts to form a liquid. The process provides a liquid stream of practically pure CO_2 free from gaseous N_2, CH_4, or H_2 at 150 bar and a gas stream at atmospheric pressure, with both streams close to ambient temperature (Baxter, 2015).

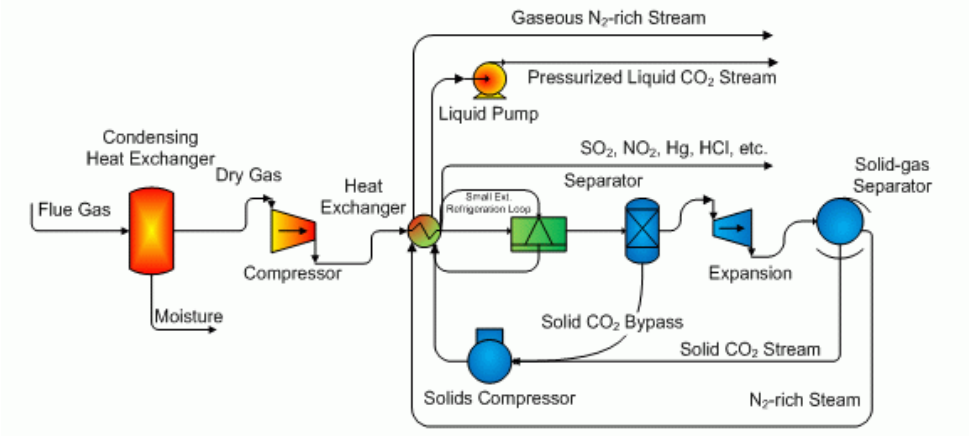

Figure 2.4: Schematic diagram of the cryogenic carbon capture (CCC) (Baxter, 2015).

The major drawbacks of this process are the amount of energy required to provide the refrigeration and highs demands on components (Wong and Bioletti, 2002). On the contrary, the cryogenic route offers a lot of advantages such as lower energy

consumption, lower costs, optional energy storage, relatively easy retrofit, lower water use, and optional criteria emission (Baxter, 2015).

2.2.4 Membranes

Membrane gas separating technology is often listed as a potential candidate for the application in post-combustion capture. Separation membranes are thin barriers, mostly based on polymeric materials that allow selective permeation of certain gasses. The membrane modules used in gas separations are spiral wound, capillary and hollow fibre and are shown schematically in Figure 2.5 (Brunetti et al., 2010).

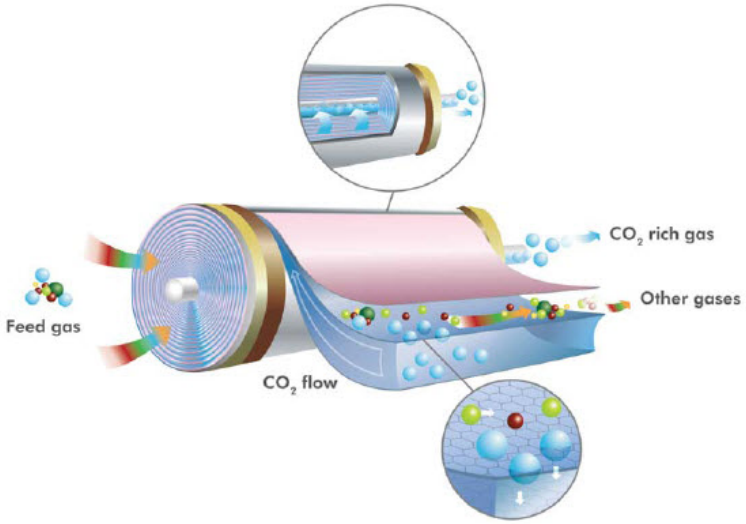

Figure 2.5: A spiral wound module showing the separation of carbon dioxide from other gases (Wong, 2016).

One of the main advantages of membrane technology is the modular design which allows them to be used in combination with small-scale modular fuel cells, representing a power plant concept for the future (Maroto-Valer, 2010a). However, it is strongly affected by the flue gas conditions (the low CO_2 concentration and pressure). This fact poses the main problem related to their limited application for CO_2 capture in post-combustion process (Leung et al., 2014).

2.2.5 Chemical Looping

The main idea of chemical looping combustion is based on the use of a chemical compound (e.g. a metal) that can be first oxidized in presence of air and then reduced when it comes into contact with the fuel. The transition metal oxide (e.g. Mn, Fe, Co, or Ni) is employed as an oxygen carrier to circulate between the two reactors. The oxide particles react with a fuel in a fluidized bed reactor producing solid metal particles and a mixture of CO_2 and H_2O. Subsequently, the reduced metal oxide is transferred to an air reactor where the metal is oxidized. The outlet gas consists of nitrogen and a reduced amount of oxygen in this case (D'Alessandro et al., 2010). The entire process is documented in Figure 2.6.

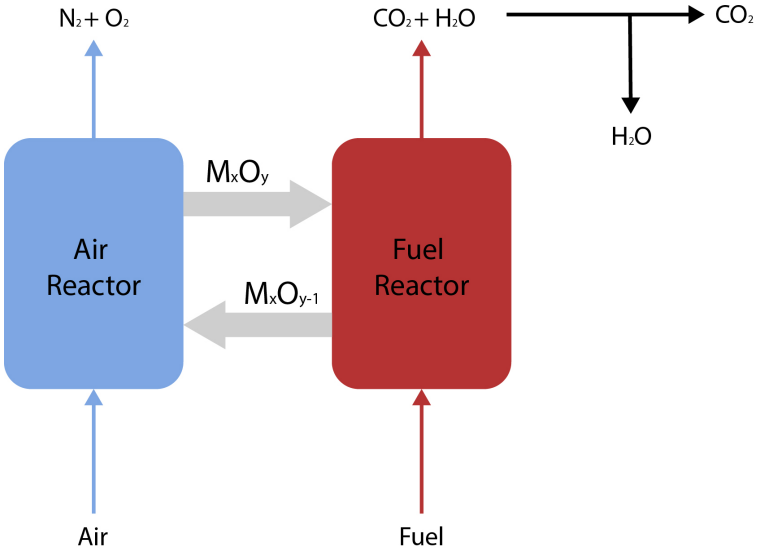

Figure 2.6: Scheme of the process of chemical looping combustion (Bermúdez et al., 2013).

The chemical looping principle may be applied either in a gas turbine cycle with pressurized oxidation and reduction reactors or in a steam turbine cycle with atmospheric pressure in the reactors (see Brandvoll and Bolland, 2002).

Work on chemical looping combustion is currently in the initial stage. The challenge is chiefly to develop suitable reactor technologies, appropriate materials and increase the performance (Metz et al., 2005).

2.2.6 Gas Hydrates

Gas hydrates are crystalline solids, in which low molecular weight guest molecules are trapped inside cages of hydrogen-bonded water molecules. Hydrate technology for gas separation will be good choice in application fields where the inlet gas has a high pressure and low temperature such as the oil and gas industry (Castellani et al., 2013).

Hybrid separations processes, which combine the advantages of hydrate crystallization with membrane technologies appears auspiciously toward the future. However, at this time the system is costly and inefficient so the rate of hydrate formation needs to be enhanced (D'Alessandro et al., 2010).

2.3 Transport of CO_2

The transport process configuration, in addition to transport specifications, depends on the capture process and the specifications from the reservoir. It must be also flexible enough to accommodate an increase in CO_2 emissions captured over time and potential changes in the end result of CO_2 capture. The challenging task is to select the appropriate specifications for the capture plant and the gas condition specification that covers the transport process (Maroto-Valer, 2010a; Al-Fattah et al., 2011).

2.3.1 CO_2 conditioning

The gas conditioning process is the interface between CO_2 capture and transport. It must be designed with respect to the particular combination of capture and transport processes. The energy requirement for the conditioning ranges typically between 90 and 120 kWh/tonne CO_2 depending on the composition and pressure of the CO_2-rich stream and the selected transport process (Aspelund and Jordal, 2007). The conditioning process is used to:

- Purify the CO_2 stream into a composition appropriate for the transport. Generally, it depends on performance of the capture/separation technology and on the characteristics of the emitting process (Al-Fattah et al., 2011).

- Remove water to avoid gas hydrates, freezing of water and corrosion. Vapor–liquid separator drums are used for this purpose. This component is considered as the simplest and most cost and energy effective way to remove the bulk of components with higher density than gaseous CO_2 (Aspelund and Jordal, 2007).

- Ensure optimal thermodynamic properties of transported CO_2 (see Figure 2.7) (Al-Fattah et al., 2011).

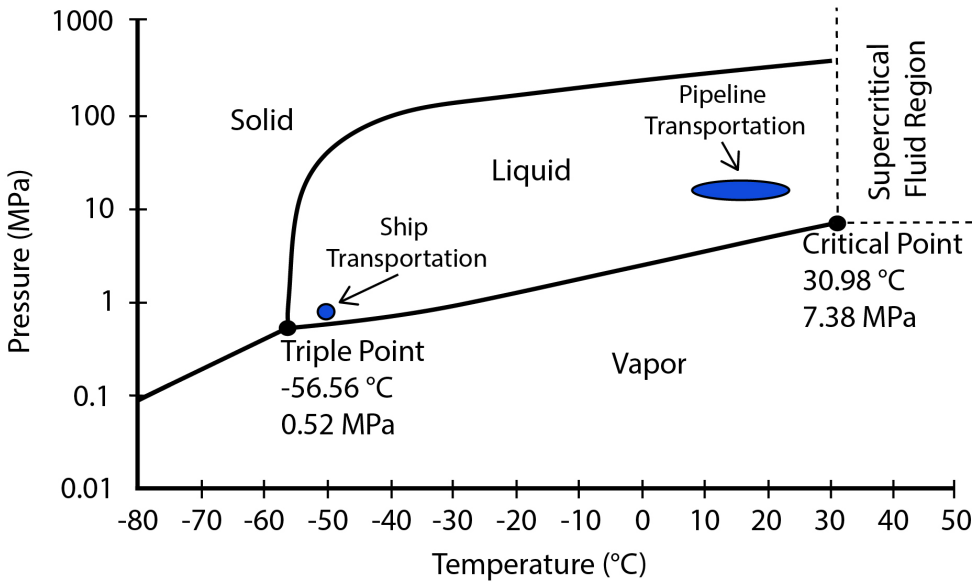

Figure 2.7: Phase diagram of CO_2 indicating the triple and critical points (Wilcox, 2012).

Generally, multistage compression showed in Figure 2.8 is used to prepare CO_2 for transport. This process brings the CO_2 to slightly above the critical pressure. Water and other harmful impurities are eliminated during the compression process. The final parameters of CO_2 must meet concentrations specified by reservoir requirements, technical/economical evaluation and rules and regulations (see e.g. Table 2.2) (Al-Fattah et al., 2011; Aspelund and Jordal, 2007).

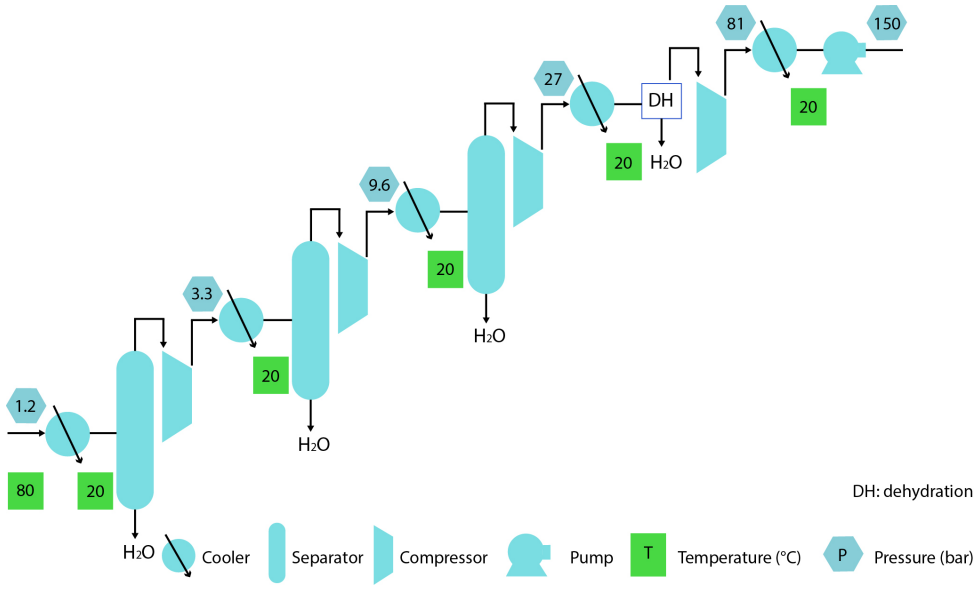

Figure 2.8: Example of CO_2 compression train (Al-Fattah et al., 2011).

2.3.2 Pipelines

Pipelines are the most common method for transporting large volumes of CO_2 over long distances. There are currently roughly 6,200 km of CO_2 pipelines in operation in the USA and Canada, transporting 30 Mt per year of CO_2 (Birol et al., 2009). To avoid two-phase flow, CO_2 should be transported in the supercritical phase, which occurs at a pressure greater than 7.38 MPa. It is recommended to transport in the interval from 70 to 150 bar where changes in compressibility can be avoided at a range of temperatures used for pipeline operation. Common design parameters for CO_2 pipeline transport are listed in Table 2.1 (Maroto-Valer, 2010a).

Table 2.1: Common design parameters for pipeline transport (Bock et al., 2003).

Parameter	Value	Units
Inlet pressure	15.2	MPa
Minimum outlet pressure	10.3	MPa
Average CO_2 temperature	25	°C
Average CO_2 density	884	kg/m^3
Average CO_2 viscosity	6.06×10^{-5}	$N \times s/m^2$
Pipeline roughness factor	4.57×10^{-5}	meters
Pipeline capacity factor	100	%
CO_2 purity in pipeline	100	%
Change in elevation	0	meters

High dryness of carbon dioxide must be ensured to prevent corrosion. The carbon-manganese steels generally used for pipelines are protected from unfavourable influence of carbon dioxide as long as the relative humidity is less than 60 % (see Rogers and Mayhew, 1980). Although impurities such as nitrogen or oxygen are not harmful, it is cost-effective to remove most of these ingredients that are shown in Table 2.2 (Maroto-Valer, 2010a; Metz et al., 2005).

Table 2.2: European Union's recommended quality specifications for pipeline transport of CO_2 (Wilcox, 2012).

Component	Concentration limit	Application
H_2O	0.03 % – 0.05 %	Free water minimization
H_2S	0.02 %	Health and safety
CO	0.2 %	Health and safety
SO_x	0.01 %	Health and safety
NO_x	0.01 %	Health and safety
O_2	<4 vol %	Aquifer storage
	<0.1 %	EOR technical limit
CH_4	<4 vol %	Aquifer storage
	<2 vol %	EOR technical limit
N_2 + Ar + H_2	<4 vol % total	

There are two basic types of pipelines. Onshore pipeline transport is a proven technology with approximately 2,400 km of large CO_2 pipelines in operation globally (Gale and Davidson, 2004). The majority of these pipelines are used to supply enhanced oil recovery (EOR) operations in the USA (see Sheng, 2013). In some cases, it appears economically advantageous to design the pipeline with booster compressor

stations every 150–300 km. On condition that CO_2 is recompressed at intervals, it allows to use pipelines with smaller diameter which are naturally cheaper. Nevertheless, there is a trade-off between lower pipe costs and the added costs of compression (see McCoy and Rubin, 2008; Bock et al., 2003). The offshore pipeline has two major differences from the onshore pipeline (see Dahowski and Dooley, 2005). First, utilization of booster stations for offshore pipelines is impractical which means offshore pipelines may require larger diameters than equivalent onshore pipelines in order to maintain pipeline pressure. The second distinction that must be taken into account is not only variable pressure between the inlet and outlet, but also the gravity head gain due to the large decrease in elevation from the shore to the outlet at –2,000 to –3,000 m (Maroto-Valer, 2010a).

2.3.3 Ship transport

By this time there have only been small tonnage ships (approx. 1,000 tons) for supplying CO_2 to the food industry and other small scale purchasers. The existing fleet is transporting CO_2 with a pressure of around 15–20 bar and a temperature of about -30°C. For larger volumes, the parameters are likely to be around 6.5 bar and -55°C (near CO_2 critical point) (Neele et al., 2014; Al-Fattah et al., 2011).

The process of CO_2 transport by ship depicted in Figure 2.9 comprises the following steps:

- CO_2 is first liquefied (by reducing the temperature) and is transitorily placed in buffer storage to align continuous capture with discrete transit of ships (Al-Fattah et al., 2011).
- Liquid CO_2 is loaded onto the ship (Metz et al., 2005).
- During the transport at sea, heat transfer from the environment through the wall of the tank will boil CO_2 and cause increase of the pressure. Therefore, the pressure level must be controlled and if needed discharge the CO_2 (Al-Fattah et al., 2011).

- Liquid CO_2 is unloaded at the target destination. It may take place at the platform itself or at a buoy or another floating installation, often called FPSO (Neele et al., 2014; Metz et al., 2005).

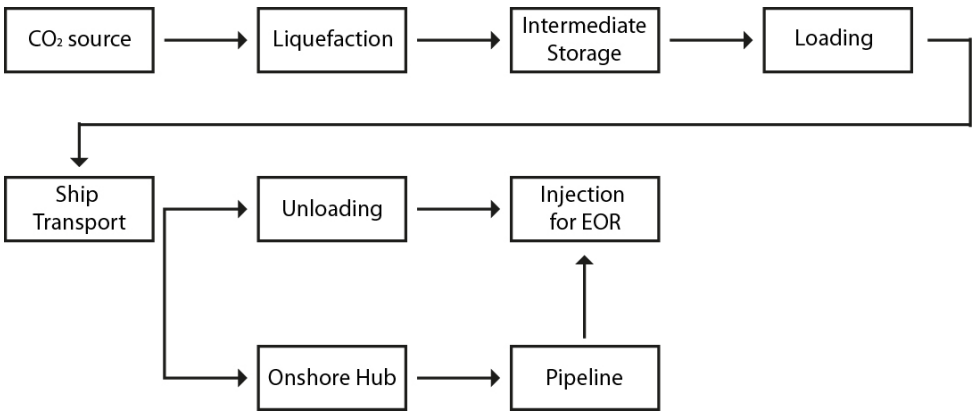

Figure 2.9: A ship-based CO_2 chain (Neele et al., 2014).

The use of ships for transporting CO_2 is in its infancy. There are only four small ships used for transport liquefied food-grade carbon dioxide around the North Sea (Metz et al., 2005). Vessel sizes range from 1,000 to 1,500 m^3 and transport pressure varies between 14 and 20 bar. These boats are inappropriate for large-scale transport of CO_2 because the lower pressure is required (Al-Fattah et al., 2011).

2.3.4 Comparison of transport by ship and pipeline

The pipeline and ship transport processes are similar and composed of the same basic building blocks. Nevertheless, the pipeline transport process is approximately 20 % more energy-efficient and is expected to have 30 % less investment costs than a liquefaction process. Although pipeline systems prevail for large quantities of CO_2, ships transport may be favoured for long-distance transport (> 500 km) and smaller volumes (Maroto-Valer, 2010a). Advantages and disadvantages of both technologies are summarized Table 2.3.

Table 2.3: Ships versus pipelines: Pros and cons (Neele et al., 2014).

Pipelines +	Pipelines -	Ships +	Ships -
Low Opex	High Capex	Low Capex	High Opex
Onshore need for compression	Relatively low flexibility	Large flexibility (volume and route)	Onshore need for intermediate storage and liquefaction plants
Can be built both onshore and offshore	Low potential for re-use	Re-use potential	
	Large sunk cost	Lower sunk cost	
		Short delivery time	

2.4 Injection processes and technology

The main task of deep-well disposal is to permanently isolate injected fluids from the biosphere. Injection towers are divided into several categories in terms of regulation and the type of waste. For each category is suitable different construction and operating system depending on the purpose (Maroto-Valer, 2010a).

First attempts of industrial waste into underground formations through injection wells date back to the 1930s by the US petroleum industry (see Clark et al., 2005). Deep-well injection facilities were executed in Russia at industrial scale. Typical examples include the Kirovo-Chepetsk Chemical combine at 1,260–1,440 m depth of injection in limestone formations and the Kalinin Atomic Power Plant at 1,200–1,400 m depth of injection in sand formations (Rybalchenko et al., 2005).

Injection well technology such as drilling or completion is due to the oil and gas industry (EOR) in highly sophisticated state nowadays. A major role in the design of injection well plays corrosion-resistant materials and injection rates. CO_2 injection well differs from gas injection well, in an oil field in downhole components which needs to be upgraded for higher pressure ratings and corrosion resistance (Maroto-Valer, 2010a).

Common injection well depicted in Figure 2.10 is equipped with two valves for well control, one for regular use and one reserved for safety shutoff. There are several constructional solutions regarding the location of the valves. They can lie externally as master valve above the wellhead or along the CO_2 supply pipeline or one is external

while the other is placed inside in the injection tubing above the double-grip packer. The purpose of the double-grip packer is to serve as a mechanical hold-down system which enables differential pressures to be held securely from both above and below the packer in the annulus between the casing and the injection tubing. It alongside maintains the pressure in the annulus. An important part of injection well is also monitoring system which controls its integrity (Maroto-Valer, 2010a; Metz et al., 2005).

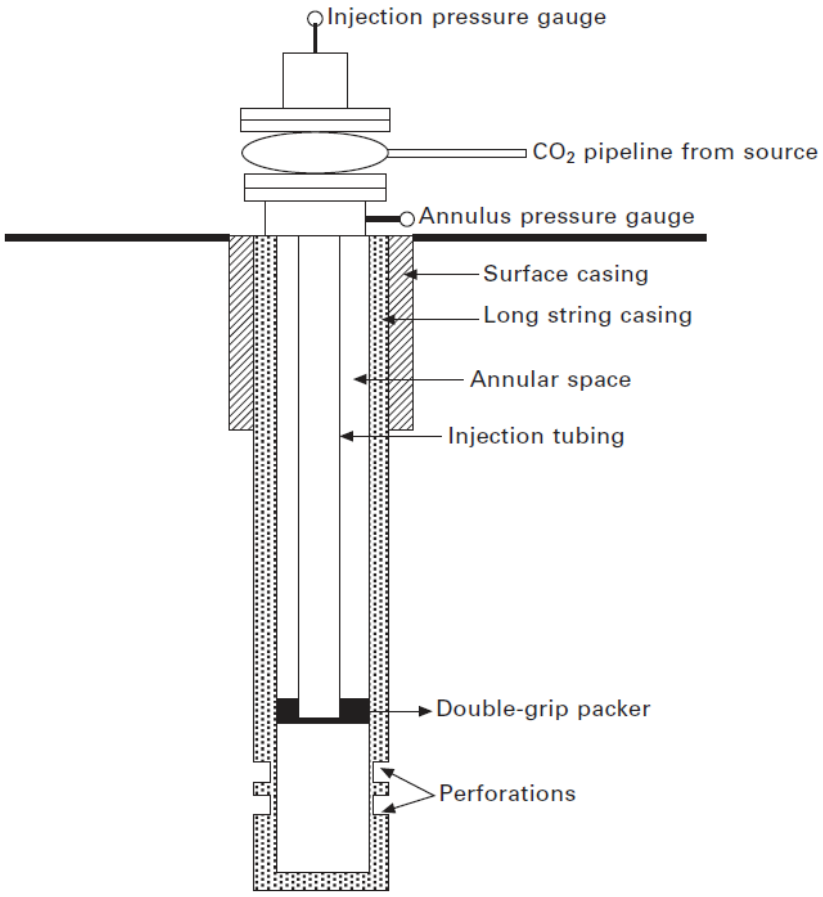

Figure 2.10: Illustration of simplified vertical CO_2 injection well (Maroto-Valer, 2010a).

2.5 Carbon Storage

2.5.1 Introduction

The key to appreciate the challenges connected with storage is an understanding of the rock into which the CO_2 is injected. There are three main deep formations which have been identified for subsurface CO_2 injection in the short-to-medium term: coal beds, oil and gas reservoirs and deep saline aquifers. It is advantageous to store CO_2 at depths below about 800–1,000 m because it has there a liquid-like density that provides the potential for efficient utilization of underground storage space in the pores of sedimentary rocks. Carbon dioxide can remain trapped underground thanks to a number of mechanisms, such as confining layer (caprock) or trapping below an impermeable. Compliance with the requirements of each selected location for carbon dioxide storage is controlled by proper and transparent process (Maroto-Valer, 2010b; Metz et al., 2005).

2.5.2 Deep saline aquifers and formations

Deep saline aquifers offer the largest storage potential (capacity is estimated between 350 and 11,000 Gt) of all the geological CO_2 storage options and are widely distributed throughout the world so it poses a great advantage in terms of costs saved on the pipeline. As a disadvantage is considered no other practical use (Birkholzer et al., 2009; White et al., 2003).

Sleipner project (see Subsection 2.7.1) holds primacy in carbon dioxide underground storing for reasons of greenhouse gas mitigation. It was built for demonstrating purpose in the Sleipner natural gas field in the North Sea off the coast of Norway. GHG mitigation policy has helped equally oriented projects because they become economically feasible on a much broader scale. In addition to this reality, there are several other field projects in the planning stages that aim to demonstrate and study CO_2 injection in deep saline aquifers (White et al., 2003). The greatest of them are shown in Table 2.4.

Table 2.4: Several current projects of CO_2 storage in saline aquifers (Leung et al., 2014).

Project name	Location	Scale*	Year of injection start	Max. CO_2 injection rate Mt/year
Sleipner	North sea, Norway	D	1996	1.0
In Salah	Krechba, Algeria	D	2004	1.3
Gorgon	Barrow Island, WA, Australia	D	2014	4.5
Latrobe Valley	Victoria, Australia	C	2015	13
Edwardsport	Indiana, USA	P	2015	1.0

*C: commercial; P: pilot; D: demonstration.

The most serious issues for sequestration in saline aquifers relate to what occurs after the CO_2 is injected. Storing these additional fluids may cause pressure changes. This fact could possibly lead to failure of the reservoir so it has been suggested that the well bottom pressure must not exceed the formation pressure by more than 9–19 %. Another possible impact of CO_2 sequestration is change in permeability of the formation induced by carbon dioxide and it might have a great impact on the rate of injection that is feasible in a given well (Birkholzer et al., 2009; White et al., 2003).

2.5.3 Oil, gas reservoirs and use for EOR & EGR

Another option for storing the captured CO_2 emissions from CCS is to inject (see Figure 2.11) the CO_2 into oil reservoirs, using it to produce additional oil. This option is called CO_2 enhanced oil recovery (CO_2-EOR) which can be way to low-carbon future. Revenues from carbon dioxide sales to the EOR industry may help to defray partially the cost of CO_2 capture from industrial sources of CO_2 (Godec et al., 2011). Another advantage provided by this technology is already built infrastructure and wells which may be used for handling CO_2 storage operations with minor or even without modifications (Li et al., 2006). CO_2-EOR has only occurred in a few regions of the U.S. and Canada. An example can be Weyburn in Saskatchewan, Canada (see Subsection 2.7.3) where CO_2 is injected from a coal gasification plant in North Dakota (Maroto-Valer, 2010b). CO_2-EOR is used with an incremental oil recovery of

7-23 % (average 13.2 %) of the original oil in place (OOIP) (Moritis, 2003). Potential benefit by CO_2-EOR ranges between 0-16 US\$/tCO_2 (Metz et al., 2005).

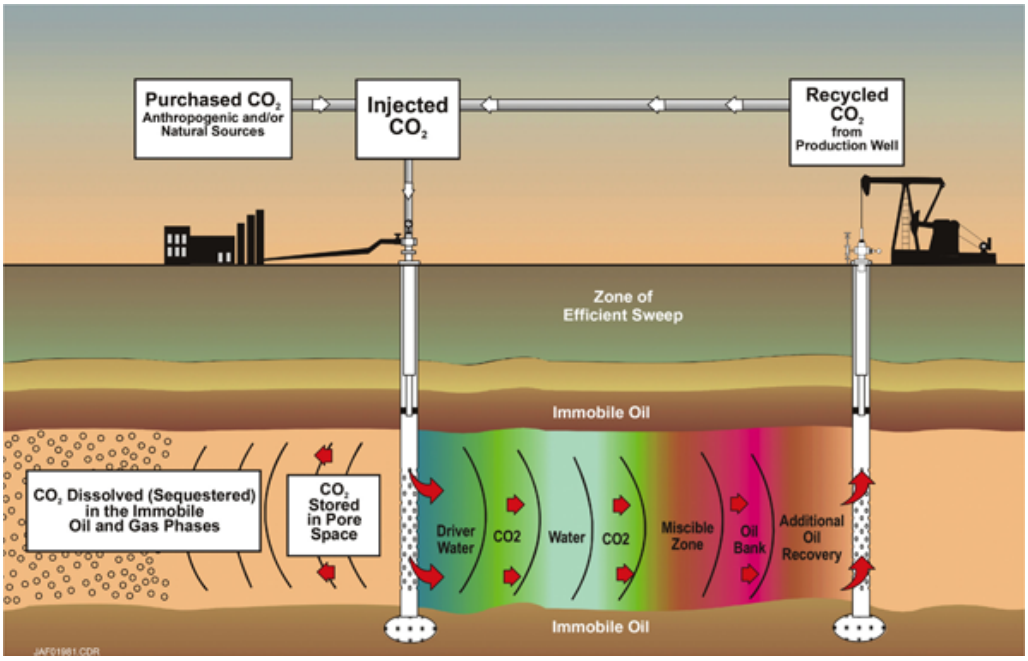

Figure 2.11: Injection of CO_2 for EOR with some storage of retained CO_2 (ARS, 2016).

CO_2 is not injected into gas reservoirs in any signification volumes nowadays. Even though, studies have demonstrated the injection of carbon dioxide accelerates natural gas production from a gas reservoir by providing repressurization (Oldenburg et al., 2001). Natural gas reservoirs are able to store more quantities of CO_2 than depleted oil reservoirs with consideration of the same volume. Gas recovery is also with recovery about 65% of initial gas in place almost about two times higher that of oil. Although, the process of CO_2-EGR is technically and economically favourable, displacement of natural gas by supercritical CO_2 still had not been properly investigated (Khan et al., 2013). Main issues are the cost of carbon dioxide, infrastructure and high primary recovery rates of many gas reservoirs. Based on estimates can CO_2-EGR provide a benefit of 4-16 US\$/tCO_2, depending on the price of gas and the effectiveness of recovery (Oldenburg et al., 2004).

2.5.4 Coal seams and use for ECBM

Coal seams are fractured porous media, characterized by a large internal surface area. They contain naturally stored methane which can be displaced by injected carbon dioxide. This technology called CO_2-enhanced coalbed methane recovery (CO_2-ECBM) allows production of relatively clean and valuable hydrocarbon. As Table 2.5 shows, the estimated storage potential of coal seams is relatively small compared to other geological formations (Masoudian, 2016).

Table 2.5: Global storage capacity for several geological sequestration options (Metz et al., 2005).

Reservoir type	Storage capacity (Gt CO_2)	
	Lower Estimate	Upper Estimate
Oil and gas fields	675	900
Un-mineable coal seams (ECBM)	3-15	200
Deep saline formations	1,000	Uncertain, but possibly 10,000

This way of CH_4 recovery has been successfully practised at Burlington Resources in New Mexico and it is planned in many other locales. Due to a lack of information, it is difficult to determine profit or costs, however, economic analyses suppose that profit would range between 12-18 US\$/tCO_2 (Metz et al., 2005). Finally, it should be mentioned that CO_2-ECBM sequestration is in the embryonic stage of development and many important questions remain unanswered and, in some cases, unasked (White et al., 2005).

2.5.5 Ocean storage

Why deep ocean storage? There are several reasons for considering that it is a suitable storage for anthropogenic CO_2. The ocean has a vast uptake capacity occupying about 70 % of the planet's area and has an average depth of about 3.8 km. This storage capacity is orders of magnitude greater than the capacity needed to absorb the CO_2 produced by burning all of the world's fossil fuel resources (Adams and Caldeira, 2008).

A number of options have been considered as injection technology for ocean storage. As illustrated in Figure 2.12, they are including introducing the CO_2 as a rising or sinking plume (see Alendal and Drange, 2001), dispersing it from a moving ship (see Ozaki et al., 2001), and creating a lake on the deep seafloor (Adams and Caldeira, 2008).

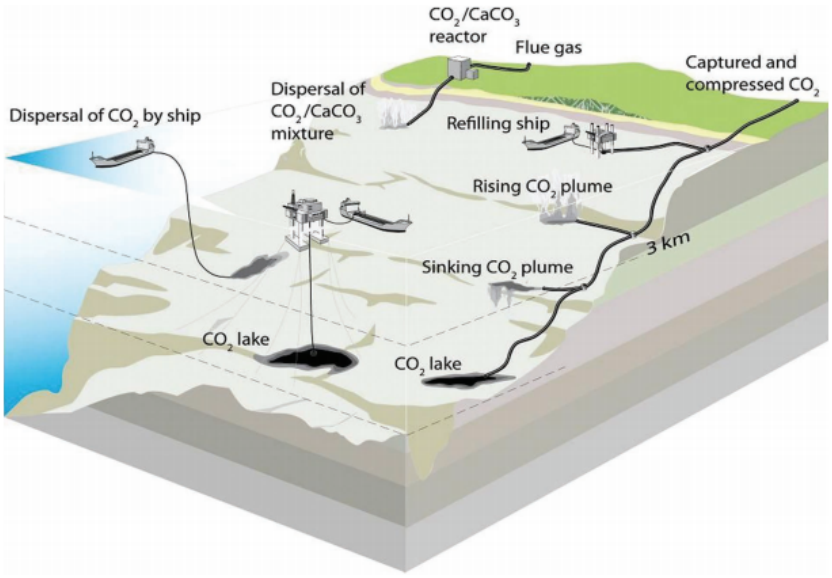

Figure 2.12: Strategies for ocean carbon sequestration (Adams and Caldeira, 2008).

There is a strong opposition by marine biologist and environmental groups to just discussed kind of storage. One of the reasons is that adding about 2,000 Gt CO_2 to the ocean would reduce the average ocean pH by about 0.1 units. PH decrease of 0.1 from the preindustrial era to today's value of 8.2 causes concern for the health of coral reefs and other organisms that use calcium carbonate in their skeletons or shells. The main task for research is to determine how much pH change might be tolerated and also additional impact of ocean storage which is still not well known (Adams and Caldeira, 2008; Maroto-Valer, 2010b).

2.5.6 Mineral carbonation

Mineral carbonation is the fixation of CO_2 as stable carbonate minerals such as calcite, magnesite, dolomite and siderite. This reaction is called silicate weathering in

nature and takes place on a geological time scale. In the case of silicate rocks, carbonation can be carried out either ex-situ which involves the aboveground carbonation of natural minerals and industrial alkaline wastes via industrial processes, or in-situ where CO_2 is injected underground under optimized conditions in silicate-rich geological formations or in alkaline aquifers. There are also other MCT routes such as biomineralization which is a process where living forms influence the precipitation of mineral materials or passive carbonation characterized by interaction of CO_2-rich fluids and ultramafic rocks (Olajire, 2013; Maroto-Valer, 2010b).

Figure 2.13: The field-scale, in situ basalt-carbonation pilot plant in Hellisheidi, Iceland (Oelkers et al., 2008).

Mineralization of CO_2 presents the most important alternative for carbon dioxide storage in underground formations. The method offers the potential for long-term, safe CO_2 storage at a reasonable price. Moreover, solid products can be used in applications ranging from land reclamation to iron and steelmaking. Despite all these advantages, there is no concept for implementation on a large scale because of the need for further research. There will be required more field-scale pilot studies like the Carbfix project showed in Figure 2.13, to better characterize the rates of mineral carbonation reactions and to determine consequences of injecting CO_2 into reactive silicate rocks (Oelkers et al., 2008; Olajire, 2013).

2.6 Economic costs

It is not easy to determine the costs of CCS technology because it depends on many factors including:

- Technical scope of the project (type of technology and whether it is situated on brownfield or greenfield sites) (Al-Fattah et al., 2011).
- Labour scope (design, type of technology and whether the plant is located in a union or non-union jurisdiction affects the labour costs) (Al-Fattah et al., 2011).
- Commercial scope (represented by owners costs such as contingencies, warranties, insurance, technical and other risks and returns on investment) (Al-Fattah et al., 2011).

2.6.1 Cost of CO_2 capture

In most projects, the costs of capturing CO_2 represent the largest component of overall CCS costs. Generally, capture costs also include the cost of purifying, compressing of carbon dioxide to a pressure suitable for pipeline or ship transport and also and expenses associated with operating and maintenance. Important factors which influence the overall cost of capture system are the time of implementation (demo phase, early or mature commercial deployment), location of the project (fuel and labour costs), technology maturity, retrofit versus new plant and of course plant size (Al-Fattah et al., 2011; Metz et al., 2005). Figure 2.14 presents CAPEX and OPEX of capture for different technologies.

To compare carbon capture with other options for reducing carbon emission, it is useful to estimate the avoided cost of CO_2 emissions (see Equation 2.1):

$$LC_{2avoided} = \frac{COE_{capture} - COE_{ref}}{E_{CO_2ref} - E_{CO_2capture}} \tag{2.1}$$

where $LC_{avoided}$ is the levelized cost of avoided CO_2 emissions (US\$/tCO_2 avoided), $COE_{capture}$ is the cost of electricity for the plant with capture (US\$/kWh), E_{CO_2ref} is the CO_2 emissions rate of the reference plant (tCO_2/kWh) and $E_{CO_2capture}$ is the CO_2 emissions rate of the capture plant (tCO_2/kWh) (Maroto-Valer, 2010a).

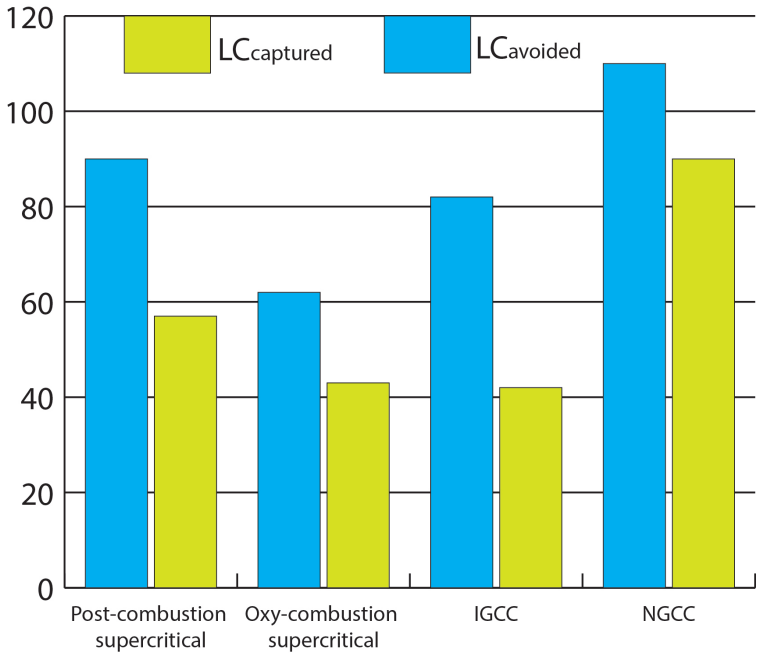

Figure 2.14: CO_2 capture costs for various technologies (Al-Fattah et al., 2011).

A similar metric is the cost of CO_2 capture (see Equation 2.2), also in US\$/tCO_2. This is useful for comparing to the market pricer of CO_2 for example for EOR:

$$LC_{2captured} = \frac{COE_{capture} - COE_{ref}}{CO_{2capture}} \tag{2.2}$$

where $LC_{captured}$ is the levelized cost of captured CO_2 emissions (US\$/tCO_2) and $CO_{2capture}$ is the quantity of CO_2 captured at the plant (tCO_2/kWh). The cost of captured CO_2 is always less than the avoided cost of CO_2 emissions because the energy required to operate the CO_2 capture system adds to the amount of carbon dioxide emitted per kWh(Maroto-Valer, 2010a; Rubin et al., 2003).

Costs of CO_2 capture processes such as cement or steel production are similar to those from fossil fuel-fired power. On the other hand, non-power applications where a relatively pure carbon dioxide stream is produced as a by-product (e.g. natural gas processing, ammonia production) are significantly cheaper due to lower demands on technology (Al-Fattah et al., 2011).

2.6.2 Cost of CO_2 transport

Several studies identify pipeline transport as the most economical method for moving large volumes of CO_2. The cost of pipeline transport is affected by construction costs (material, labour, and booster stations), operation and maintenance costs (monitoring, maintenance and energy) and other costs (design, insurance, fees, right-of-way) (Metz et al., 2005). Significant cost impacts may have special land conditions like heavily populated areas, protected areas such as national parks or crossing major watercourses. Estimates in accordance with Figure 2.15 show that offshore pipelines are about 40 % to 70 % more costly than onshore pipes of the same size. (Al-Fattah et al., 2011).

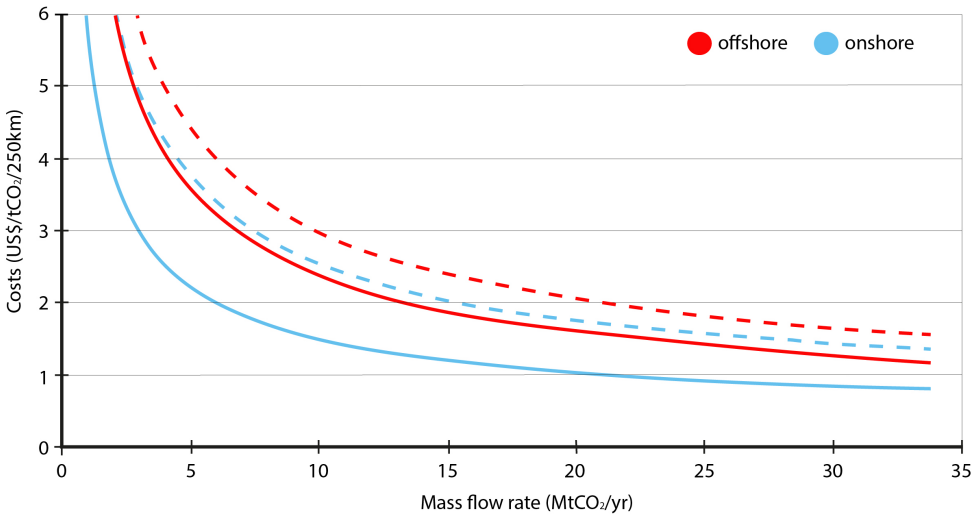

Figure 2.15: CO_2 transport costs range for onshore and offshore pipelines per 250 km, "common" terrain conditions. The figure shows low (solid lines) and high ranges (dotted lines) (Metz et al., 2005).

Large tankers may be cost competitive transport option for longer distances at sea. For this kind of transport are the main cost elements tankers themselves (or chartes costs), loading and unloading facilities, intermediate storage facilities, harbour fees and bunker fuel (Metz et al., 2005). Cost estimates of tankers are largely based on existing LPG ships that operate under similar conditions to those required for carbon dioxide transport (Aspelund et al., 2006). The costs of CO_2 tankers are estimated at US$ 34 million for ships of 10,000 tonnes, US$ 58 million for 30,000–tonne vessels

and US$ 82 million for ships with a capacity of 50,000 tonnes (Metz et al., 2005).

2.6.3 Cost of CO_2 storage

There is a significant range and variability of costs due to site-specific factors like the reservoir depth, onshore versus offshore and the geological characteristics of the storage formation (e.g. permeability, thickness, etc.) (Metz et al., 2005). The most expensive component is usually a drilling well. The costs of individual wells range from about US$ 200,000 for some onshore sites to US$ 25 million for offshore horizontal wells (Bock et al., 2003). Overall storage costs of geological formations summarizes Table 2.6. Although uncertainty still remains, there were a lot of research which has allowed a more detailed breakdown of costs associated with geologic storage (Rubin et al., 2015).

Table 2.6: Storage costs in 2009 EUR/tCO_2 (ZEP, 2011).

Reservoir type	On/Offshore	Low	Medium	High
Depleted O&G Field – reusing wells	Onshore	1	3	7
Depleted O&G Field – no reusing wells	Onshore	1	4	10
Saline Formations	Onshore	2	5	12
Depleted O&G Field – reusing wells	Offshore	2	6	9
Depleted O&G Field – no reusing wells	Offshore	3	10	14
Saline Formations	Offshore	6	14	20

The costs of ocean CO_2 storage depend on three major components: tank storage of CO_2, shipping of CO_2 and injection platform pipe with nozzle for offshore injection platform or injection ship, pipe and nozzle for injection ship. Costs comparison of these two technologies offers Table 2.7 (Metz et al., 2005). At a distance up to 100 km it is preferable to use pipeline running on the see floor to an injection nozzle. CO_2 transported either 100 or 500 km by a pipeline for injection at a depth of 3,000 m at a cost of 6.2 US$/t$CO_2$ net stored (100 km case) to 31.1 US$/t$CO_2$ net stored (500 km case) (Akai et al., 2004).

Table 2.7: Ocean storage cost estimate for CO_2 transport and injection from a floating platform (depth of 3,000 m) and from a moving ship (depth of 2,500 m) (Metz et al., 2005).

Ship transport distance	Injection platform		Injection ship	
	100	500	100	500
Onshore CO_2, Storage [1]	3.3	3.3	2.2	2.2
Ship transport to injection platform [1]	2.9	4.2	3.9	5.3
Injection platform, pipe and nozzle [1]	5.3	5.3	7.7	7.7
Ocean storage cost [1]	11.5	12.8	13.8	15.2
Ocean storage cost [2]	11.9	13.2	14.2	15.7

[1] (US$/$tCO_2$, shipped)
[2] (US$/$tCO_2$, net stored)

Mineral carbonation is still in its R&D phase, so costs are difficult to determine. However, several studies claim the total cost of mineral carbonation is approximately 105 US$/$tCO_2$ avoided with no lingering unknowns (Olajire, 2013). Currently, the expenditure of this storage method appears to be enormous and must be reduced by additional research (Metz et al., 2005).

2.7 CCS Projects

Although many of component technologies for CCS are fairly prepared, there are still no fully integrated commercial applications. Nevertheless, a number of pilot-scale CCS projets were constructed around the world. World governments and energy corporations are focusing on widespread deployment of CCS technologies in the near future. As an example of the CCS projects development in Europe can serve European Energy Programme for Recovery (EEPR) and NER300 programme. Near Zero Emission Coal (NZEC) is another CCS project concluded between China and EU. Under the supervision of Global Carbon Capture and Storage Institute (GCCSI), the G8 countries have committed to the development of 20 large-scale CCS projects to be operational by 2020. The Regional Carbon Sequestration Partnerships (RCSP) was founded in order to help determine the best approaches for capturing and storing GHG in the USA. Currently, the development phase (2008-2017) which conducts large-volume carbon storage tests is under way (Maroto-Valer, 2010a).

2.7.1 Sleipner

The Sleipner Project operated by oil company Statoil in the North Sea is the first commercial-scale project dedicated to geological CO_2 storage in a saline formation. Since 1996, approximately 1 Mt CO_2 (about 9 %) is injected from offshore gas field Sleipner revealed in Figure 2.16 into a salt water containing sand layer, called the Utsira formation, which lies 1000 m below sea bottom. Although this saline formation has a plentiful storage capacity, on the order of 1-10 Gt CO_2, it is expected to store 20 Mt CO_2 over the lifetime of the project (Torp and Gale, 2004; Metz et al., 2005).

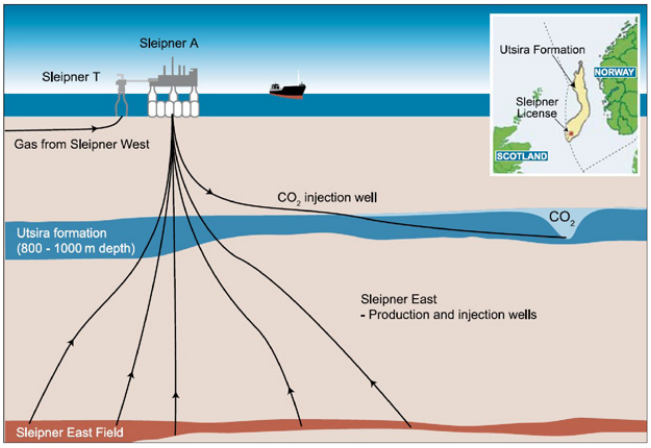

Figure 2.16: Simplified diagram of the Sleipner CO_2 Storage Project (Metz et al., 2005).

2.7.2 In Salah

The In Salah CO_2 Storage project in central Algeria has been a highly informative demonstration project which has built up a wealth of experience highly relevant to CCS projects worldwide. Carbon dioxide (1-10 %) contained in several gas fields is removed from the gas production stream in a central gas processing facility to meet the export specification of 0.3 % CO_2 and then it is compressed, transported and stored underground in the 1,800 m deep Carboniferous sandstone unit up to 1.2 MtCO_2/yr at the Krechba field (Ringrose et al., 2013).

As shown in Figure 2.17, three long-reach horizontal injection wells (up to 1.5 km) are used to inject the CO_2 into the down-dip aquifer leg of the gas reservoir. Injection

was initiated in April 2004 and since then over 3.8 million tonnes of CO_2 have been stored. However, over the life of the project, it is estimated that 17 Mt CO_2 will be geologically stored (Ringrose et al., 2013; Metz et al., 2005).

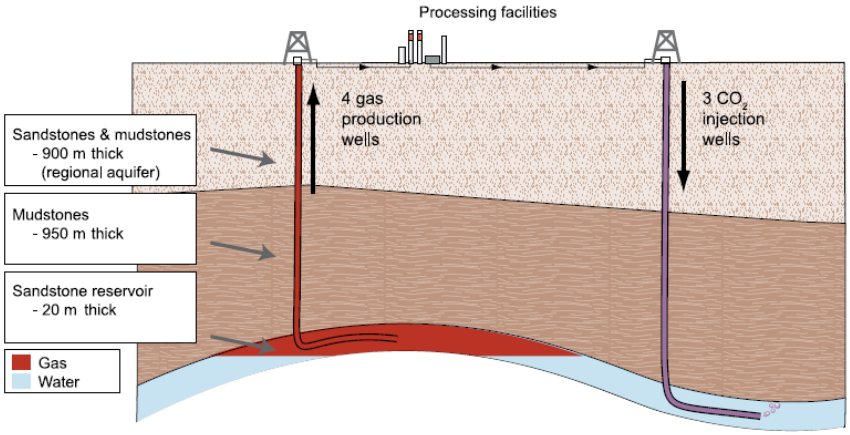

Figure 2.17: Schematic of the In Salah Gas Project, Algeria (Metz et al., 2005).

2.7.3 Weyburn

The Weyburn large-scale commercial CO_2-EOR project is located in Prairie Province of Saskatchewan, Canada. Carbon dioxide is obtained from the Dakota Gasification Company, near Beulah ND and transported 320 km via pipeline depicted in Figure 2.18 to the Weyburn. The purpose is to increase recovery of oil from the carbonate Midale Beds of the Mississippian Charles Formation, where about 3 billion m^3 of supercritical CO_2 have been injected since 2000 at a rate of 5,000 t/day (Riding, 2006; Maroto-Valer, 2010a).

Currently, about 10,063 barrels per day of incremental oil are produced from the field. The project also serves to monitor dynamic reservoir response and study effective trapping mechanisms, seals, hydraulic isolation, hydrogeological regime and pathways for migration along faults and fractures (Preston et al., 2009).

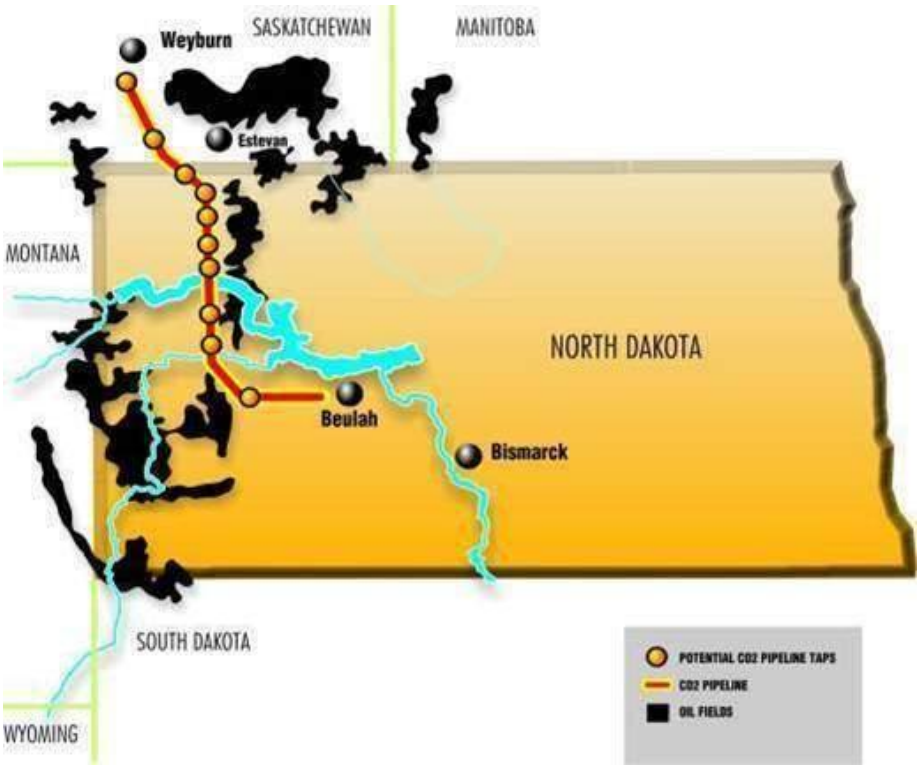

Figure 2.18: Map of international CO_2 pipeline between Beulah, ND, USA and Weyburn, SK, CAN (DGC, 2016).

2.7.4 Schwarze-Pumpe

In 2005, Vattenfall has constructed the 30 MW experimental large-scale pilot test facility depicted in Figure 2.19 for detailed investigation of the oxyfuel firing process. The plant is located south-east of Berlin in Germany near the existing lignite-fired 1,600 MW power plant (Anheden et al., 2011).

The results have proven that operation in Oxyfuel mode is manageable. It was demonstrated that high level of CO_2 purity can be obtained, due to extensive cleaning in the pilot CO_2 purification unit. All emission limits could be met as well and projected parameters regarding separation efficiency and carbon dioxide purity have been achieved. The attained capture rate is greater than 90 % so more than 90 % of CO_2 can be separated from the flue gas which enters the liquefaction process. Further tests are planned with the aim of optimization the operating parameters, tests of different burner designs and investigation of the effects of variations in fuel

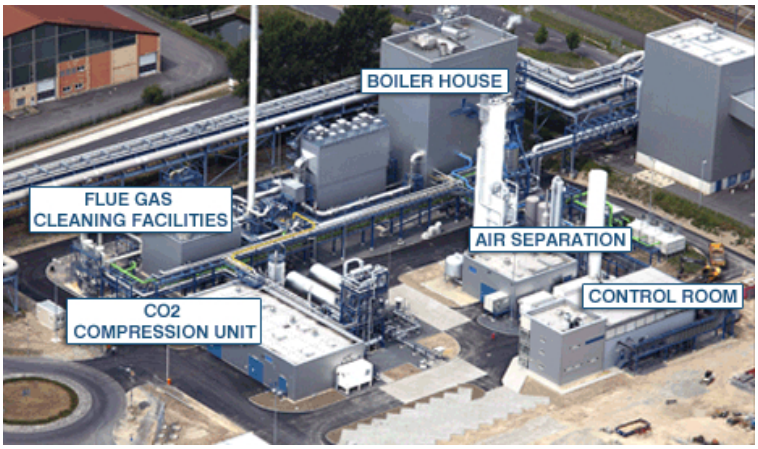

Figure 2.19: Coal carbon capture and storage site at Schwarze Pumpe, Germany (Vattenfall, 2016).

quality (Anheden et al., 2011; Metz et al., 2005).

2.8 Conclusion

Carbon capture and storage is an essential option to tackle increasing CO_2 emissions at present and in the near future. However, today's trend shows a slowdown in the planning of large-scale CCS projects and many existing projects have been stopped. The main problems hindering expansion of CCS are not surprisingly technical, but economic and social. The fact that there are no binding obligations or imposed high fines for emitting CO_2 rank among them. The noticeable increase of electricity prices caused by CCS implementation is also considered as a substantive drawback. Last but not least, the risks associated with CO_2 storage are not adequately explained and understood by the public. For these reasons, it is necessary to create conditions supporting climate change mitigation in the long run. Another indispensable step is to start public discussion led by trusted stakeholders, including NGOs and other CCS interested organisations which will explain this technology.

Chapter 3

Compressed Air Energy Storage

The increasing need to harness the renewable energy (RE) is an indisputable trend in recent years. Nevertheless, one major problem stands in the way - RE cannot steadily provide power. Thus, energy storage technologies are gaining a great deal of attention. They are providing technical viability and economic feasibility of RE and play a significant role in achieving load leveling. Along pumped hydro storage, compressed air energy storage (CAES) is considered to be one of the most promising technology for large scale storage applications. This progressive technology is described in the next chapter.

3.1 General Concept

The storage is carried out due to electrically driven compressors, which convert the electric energy into energy of pressurized air during lowcost off-peak periods. The medium is stored in various CAS volumes (see Subsection 3.2) at a high pressure. This high-pressure air is released in the case of demand to generate electricity by expansion of the air through an air turbine. The entire process is illustrated in Figure 3.1 (Venkataramani et al., 2016; Budt et al., 2016).

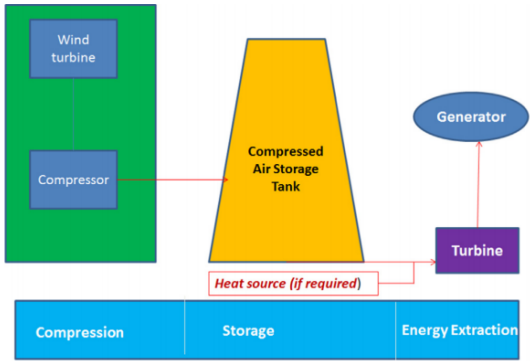

Figure 3.1: Flow diagram of CAES technology (Venkataramani et al., 2016).

Although a huge variety of dissimilar CAES concepts exists, they can be classified under three types based on air storage and heat utilization. Figure 3.2 depicts them as adiabatic, diabatic, and isothermal (Venkataramani et al., 2016).

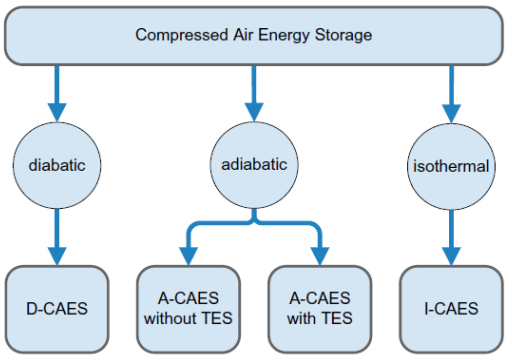

Figure 3.2: CAES concepts classified by their change of state: (D(diabatic)-, A(adiabatic)-, I(isothermal)-CAES) (Budt et al., 2016).

3.1.1 Diabatic

The compressed air (44-70 bar) is cooled down to near ambient temperature via intercoolers and then stored e.g. in underground caverns. During peak periods, the pre-compressed air from the storage cavern is preheated through a heat recuperator, mixed with natural gas or oil and subsequently burnt together in a combustion chamber (approx. 550 °C). This solution entails the advantage of lower compressed air energy losses. Finally, the mixture expands through a multistage coupled turbine-

generator (Ibrahim et al., 2015; Loose, 2011). Two large-scale plants using D-CAES are in operation at present: Huntorf plant in Germany (see Subsection 3.3.1) and McIntosh plant in Alabama, USA (see Subsection 3.3.2) (Budt et al., 2016).

3.1.2 Adiabatic

A-CAES unlike D-CAES does not need fuel to heat the expanding air because it stores and reuse the heat produced during the compression. As shown in Figure 3.3, this can be theoretically realized with or without TES device. This facility is used for storing thermal energy in the form of heat or cold when it is excessive for reuse later when it is scarce (Helsingen, 2015).

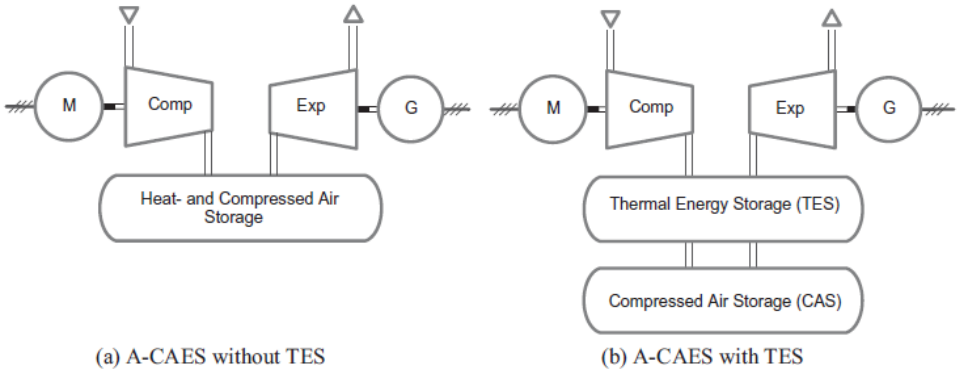

Figure 3.3: Basic methods of A-CAES (Wolf, 2011).

A-CAES without thermal energy storage (TES) is based on storage the hot air itself inside a combined thermal energy and compressed air storage volume. This technology involves major drawback in the form of a high requirement on material temperature resistance. Most of the CAS are not able to withstand temperatures about 277 °C. This fact leads to relatively low storage pressures and consequently to reduced energy densities. In the final analysis, above-mentioned type of A-CAES has only been realized in laboratory conditions and the chance for commercial use is almost impossible in the near future (Wolf, 2011; Budt et al., 2016).

Thanks to using TES device, much higher final pressures (typically at least 60 bar) can be achieved and higher energy densities can be accomplished. As demonstrated in Figure 3.4, the crucial parameter is selected storage temperature which has great

influence on cycle efficiency and operating behaviour of the whole plant (Budt et al., 2016). Of its value, three process types can be distinguished:

- High-temperature processes reaching storage temperatures above 400 °C (Budt et al., 2016). This category is represented by advanced adiabatic compressed air energy storage (AA-CAES) (see Bullough et al., 2004).
- Medium-temperature processes where storage temperatures range from 200 °C to 400 °C (Budt et al., 2016).
- Low-temperature processes with storage temperatures maintained below 200 °C (Budt et al., 2016).

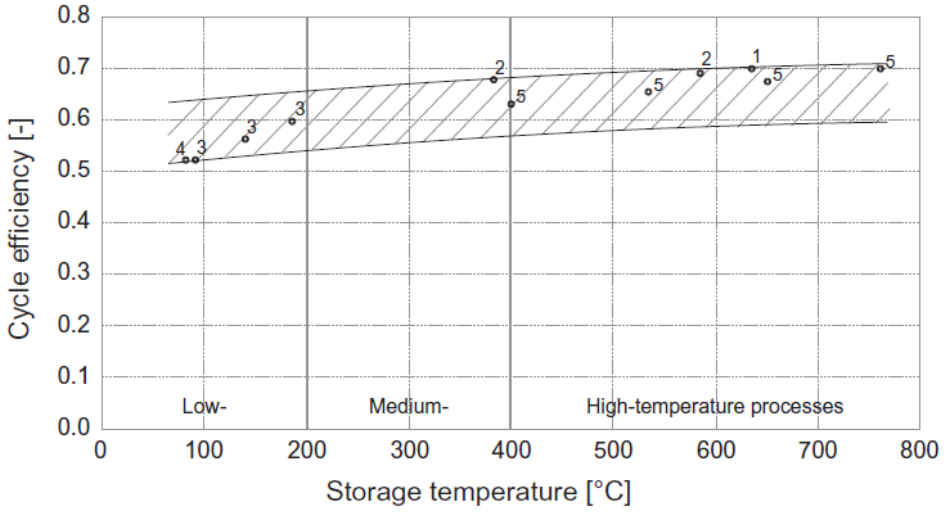

Figure 3.4: Dependence of cycle efficiencies at the storage temperature (Wolf and Budt, 2014).

Currently, two projects are in the planning phase; the ADELE project situated in Germany and the ALECAES project located in Switzerland (Power, 2012; Alaceas, 2015).

3.1.3 Isothermal

Isothermal CAES (I-CAES) works by compressing and expanding air at near constant and close to ambient temperature which reaches high yields without external heat

exchangers. This technique provides an improvement in system efficiency ranging value from 70 % to 80 % provides fuel-free operation, and reduces thermal stress on equipment (Sandén, 2014; Kim et al., 2012). Currently, three different technological processes presented in Figure 3.5 are in development:

- Gas compression with C-HyPES method is achieved using pumping a liquid (e.g. hydraulic oil) into the storage tank. When electricity is needed, the gas pressure is discharged by letting the liquid flow in opposite direction through the pump turbine (P/T), which now serves as a turbine driving the generator (Wolf, 2011). The reason for zero-commercial application is low energy density, but investigation is under way in the scientific sphere (Lemofouet-Gatsi, 2006).

- The open cycle concept (O-HyPES) is based on the air compression by a liquid piston before entering the CAS at high pressure. The liquid is pumped into and out of CAS with two alternating cylinders and a cyclic air supply, release is ensured by a system of valves. The benefit which stems from applying a liquid as working medium is higher energy densities (Wolf, 2011). This principle is exploited in pilot plant (Texas, 2012) developed by General Compression company which produces power of 2 MW (Budt et al., 2016).

- Charging and discharging power of above-mentioned concepts are restricted by the heat exchange surface formed by the liquid surface in contact with the gas. This limitation can be surpassed by spraying water into the compression chamber, which causes a significant increase of water surface touching the gas (Budt et al., 2016). Companies SutstainX and LightSail Energy constructed two pilot plants in 2013, which are already in operational mode generating power of 1.5 MW and 2 MW, respectively (Helsingen, 2015; Ibrahim et al., 2015).

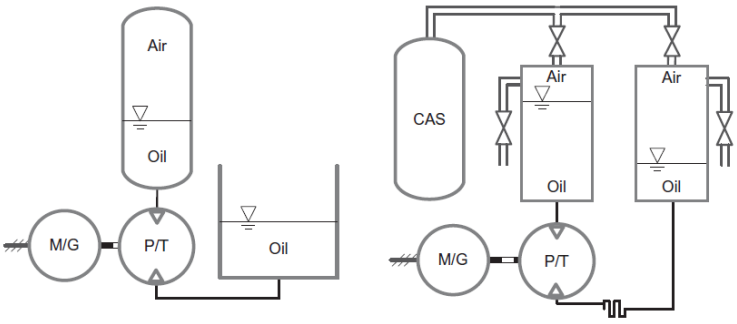

Figure 3.5: Process scheme of a C-HyPES (left) and an O-HyPES (right) (Wolf, 2011).

3.2 Compressed Air Storage

Compressed air can be stored above- and underground. For the application of underground CAS each underground cavity, which is able to withstand the needed pressure and which is dense enough to prevent air from leakage can be used (Eckroad and Gyuk, 2003; Budt et al., 2016). As examples may serve salt, hard rock and porous caverns, gas fields or mine shafts. Underground storage is cost efficient for large installations, on the contrary, there is pressure difference limitation due to rock mechanic stability (Sandén, 2014; Budt et al., 2016).

Aboveground CAS can be done in pressure containers, tanks and pipes. Even concrete storage volumes are possible considering the lower final pressures. The major benefit is location-independent installation but there are also drawbacks such as need for pressure regulation which stems from high pressure differences. The analysis also claims that this solution is about five times more expensive than underground storage and with a smaller storage capacity (Helsingen, 2015; Budt et al., 2016).

3.2.1 Isochoric storage

As Figure 3.6 shows, the first option for CAS is at constant volume (isochoric) which is considered as the simplest ones conceptually. Commonly, steel pressure vessel or, at large scale, a salt cavern is used. The facility is composed of one or more fixed shape volumes connected by some arrangement of pipes. The major drawback is high

demand on compression and expansion machinery resistance to changing pressure. They are therefore not operating in their design pressure ratio, which results in lower efficiencies (Garvey and Pimm, 2016; Budt et al., 2016).

3.2.2 Isobaric storage

Another method is isobaric CAS which requires a varying volume to maintain pressure at a constant level during charging and discharging. Compressor and expander working at the same two pressures are optimized for one single design point which gives rise to lower requirements for machinery. Although realization is comparatively complex and not widespread, it can be technically implemented using a hydraulically compensated reservoir where pressure is kept approximately constant by a second reservoir of liquid at elevated geodetic height as depicted in Figure 3.6 (Garvey and Pimm, 2016; Budt et al., 2016).

3.2.3 Cryogenic storage

The last option for storing compressed air is called liquid air energy storage (LAES) (see Figure 3.6). This technology is installable location-independent and has low investment costs. However, there is demand on liquefaction of the air (Budt et al., 2016). LAES is mentioned just by reason of completeness. Detailed information can be found in further literature (see Chino and Araki, 2000; Morgan et al., 2015).

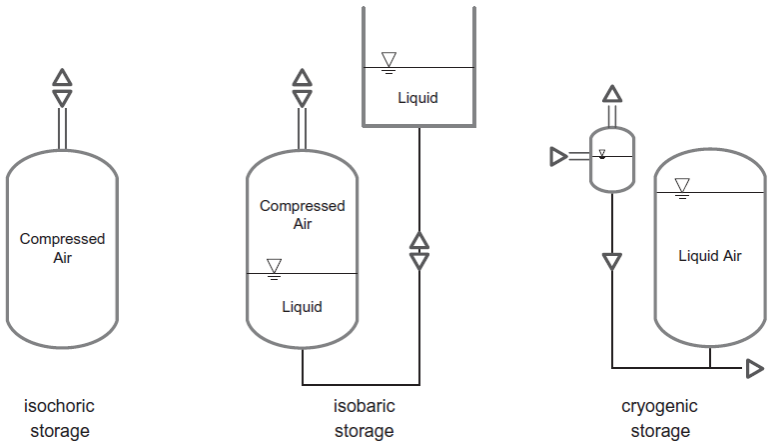

Figure 3.6: Different types of air storage devices (Wolf, 2011).

3.3 CAES Projects

Although the fundamental idea to store electrical energy by means of compressed air dates back to the early 1940s, it was not developed due to the lack of necessity for grid connected energy storage until the late 1960s. The situation has changed due to need of economic optimization by transferring cheaper baseload power toward peak hours. The development resulted in a construction of Huntorf and McIntosh power plants (see Subsection 3.3.1 and Subsection 3.3.2, respectively) (Kalhammer and Schneider, 1976; Budt et al., 2016). Another great impulse came with the progress in renewable energies such as wind and photovoltaics. Therefore the need for balancing supply of intermittent renewable energy is the main driver toward R&D on CAES technology at the moment (Lund and Salgi, 2009). A complete overview of R&D projects relating to CAES is available in Figure 3.7.

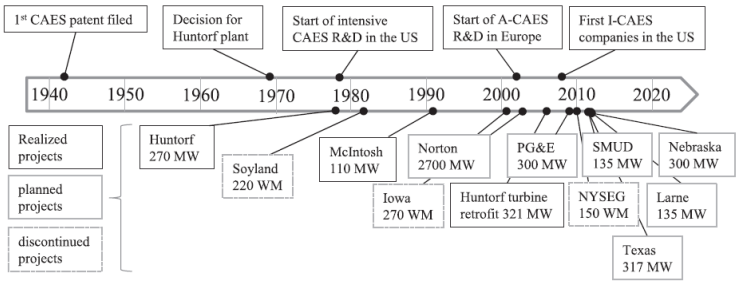

Figure 3.7: Timeline of CAES R&D and largest installations (Budt et al., 2016).

3.3.1 Huntorf plant

The Huntorf plant was built as the first of its kind in 1979 in Niedersachsen, Germany. The plant using D-CAES (see Subsection 3.1.1) operates on the same principle as traditional pump storage plants. The air is pumped into two salt caverns being cycled between approximately 46 and 72 bar, with a total storage volume of about 310,000 m^3. This solution warrants high availability by facilitating plant operation even when one of the caverns is being maintained (Crotogino et al., 2001; Budt et al., 2016).

Figure 3.8 illustrates process scheme of Huntorf plant which is described in the

following sentences. The air leaving the cavern in expansion mode is first throttled down to a constant pressure about 42 bar before entering the high pressure (HP) combustion chamber (1). Downstream of the HP combustion chamber (2), the air is now heated due to the HP combustion chamber up to 490 °C and expanded down to about 13 bar in the HP turbine (3). Under these conditions, the air is heated up again to 945 °C in the low pressure (LP) combustion chamber (4) before entering the LP turbine (5) (Budt et al., 2016; Radgen, 2008).

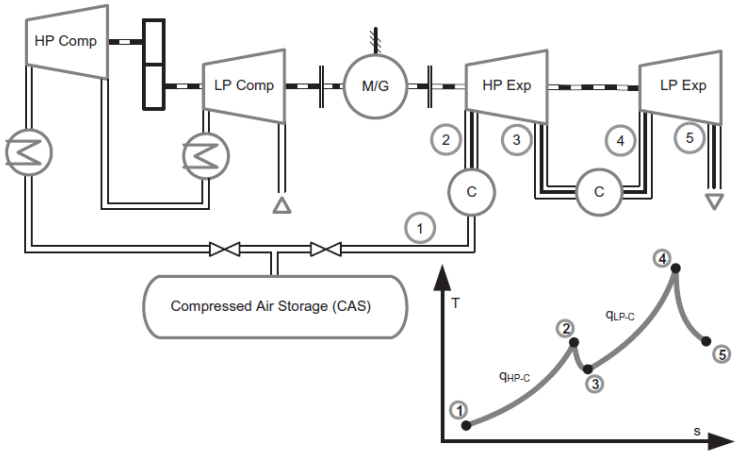

Figure 3.8: Process scheme and T,s-diagram of the expansion process of the Huntorf plant (Wolf, 2011).

The Huntorf project is unique because of first implemented features such as high pressure combustion chamber, high pressure expansion turbine and gas turbine with fast startup capability. Currently, the plant serves as a reserve facility and provides internal portfolio optimization (Radgen, 2008).

3.3.2 McIntosh plant

In 1991, 13 years after the completion of the Huntorf plant, a second large scale D-CAES plant was realized in McIntosh, Alabama (Collins, 1993). The basic arrangement is substantially the same as in the Huntorf plant. However, the CAS consists of only one large salt cavern with a total volume of 538,000 m^3 (Nakhamkin et al., 1992).

As process scheme depicted in Figure 3.9 shows, usage of an exhaust-heat recuperator represents the main difference and amelioration compared to Huntorf. Hot exhaust gasses produced during expansion mode in LP expander (370 °C) are used to preheat the compressed air (295 °C) before it enters the combustion chamber (Mason and Archer, 2012; Radgen, 2008). This technical solution reduces the fuel consumption by approximately 22-25 % (Luo et al., 2015).

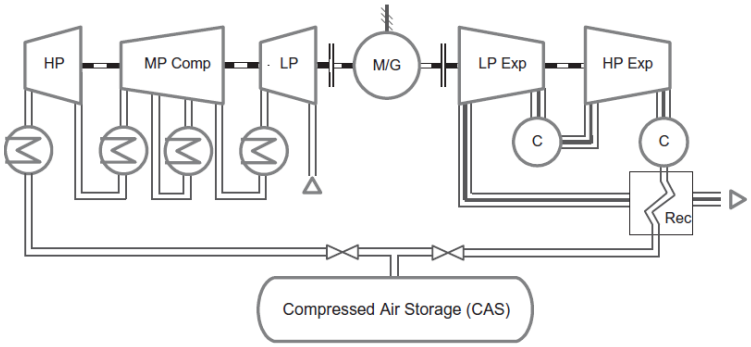

Figure 3.9: Process scheme and T-s diagram of the expansion process of the Huntorf plant (Wolf, 2011).

3.3.3 Comparison of Huntorf and McIntosh plants

Figure 3.10 offers a comparative overview using T-s diagrams of the expansion process of the McIntosh plant (black line) and Huntorf plant (grey line).

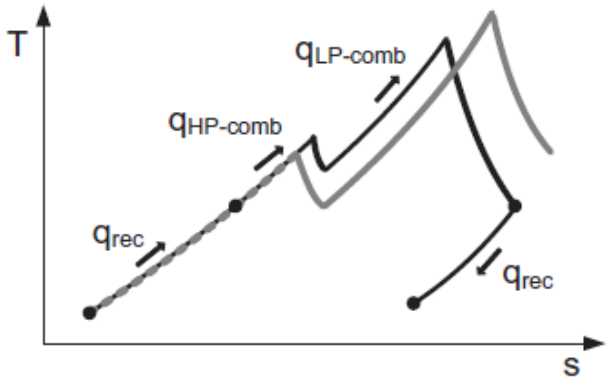

Figure 3.10: T,s-diagrams of the expansion process of McIntosh (black line) and Huntorf (grey line) (Budt et al., 2016).

Two crucial differences are visible at the sight of Table 3.1. First of all, the McIntosh cycle efficiency is significantly higher than efficiency of the Huntorf plant, reaching 54 % instead of 42 %. The major reason for the big difference in round-trip efficiency of the two plants is application of a recuperator which is completely omitted in the Huntorf plant (Budt et al., 2016; Luo et al., 2015). The second distinction is the purpose for which the plants were constructed. As the charging and discharging period in Table 3.1 shows, McIntosh was designed to perform load shifting on a weekly basis (Pollak, 1994). On the other hand, Huntorf plant was chiefly designed to provide reserve power and blackstart capability (Hoffeins and Mohmeyer, 1986).

Table 3.1: Comparison of technical parameters of operating D-CAES plants (Venkataramani et al., 2016; Budt et al., 2016).

	Huntorf	McIntosh
Plant		
Cycle efficiency	0.42	0.54
Plant capacity	290 MW	110 MW
Compression		
Compression air flow	107 kg/s	93 kg/s
Max. el. input power	60 MW	50 MW
Compressor units	2	4
Charging time (at full load)	8 h	38 h
Storage		
Geology	Salt	Salt
Number of caverns	2	1
Cavern pressure range	46–72 bar	46-75 bar
Cavern volume	310,000 m^3	538,000 m^3
Expansion		
Type of fuel	Gas	Gas/Oil
Discharging time (at full load)	2 h	24 h
Max. mass flow rate	455 kg/s	154 kg/s
HP turbine inlet	41.3 bar/490 °C	42 bar/538 °C
ND turbine inlet	12.8 bar/945 °C	15 bar/871 °C

3.4 Conclusion

Although numerous advantages were presented in the chapter, compressed air energy storage is not widely implemented. Lower cycle efficiencies than PHES or batteries and the negative impact on the profitability of grid connected storage are just some of the reasons that cause the technology issues to penetrate the market. Difficult prediction of the CAES implementation costs is another serious disadvantage. Despite the above mentioned drawbacks, it is almost impossible to imagine the development of renewable energy without the storage technologies in the coming years. Therefore the investment and development of this technology are naturally expected.

Chapter 4

Model of Energy Storage Technology

This chapter demonstrates a functional model of energy storage. The experiment served for developing of creative thinking and solving problems associated with the construction, manufacturing technology as well. Emphasis was placed on the self-reliant manufacture of components and building electronic circuits. This goal was realized by assembled devices such as 3D printer or Shapeoko (see Appendix A). Lathe and drill press was also used.

4.1 Introduction

As shown in Figure 4.1 and in Figure 4.9, the model consists of two basic parts – centrifugal compressor and Tesla turbine. The compressor engine would be ideally powered by a wind turbine. However, it is connected to 12 V source because of the ambient conditions. The compressed air flows from radial compressor into the air tank. Prevent of backflow is ensured by a valve. The solenoid valve is placed at the tank outlet. It is opened via relay at the set pressure detected by a sensor and allows a compressed air to flow to the Tesla turbine. This causes discs rotation and creation of torque on the shaft which is converted to a voltage via flexible coupling and power generator. Subsequently, voltage is stabilized, directed and turns on the bulb.

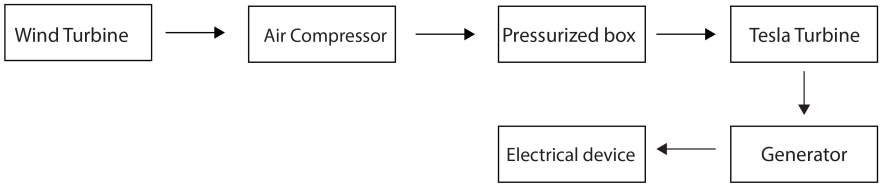

Figure 4.1: Block diagram of energy storage via compressed air.

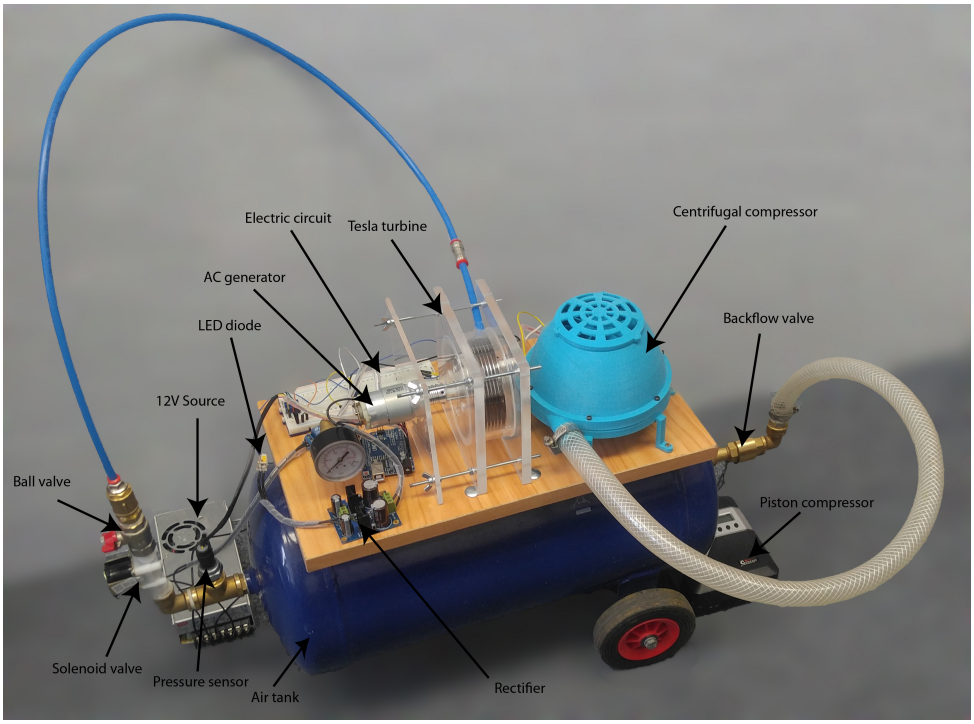

Figure 4.2: Self-assembled model of CAES technology.

4.2 Impeller

An impeller is a rotating component of a centrifugal compressor which transfers energy from the driving engine to the fluid. It is usually made of steel, iron or bronze. Nevertheless, ABS plastic is used in this case. This component is composed of open inlet through which the incoming fluid flows, blades for pushing the fluid and an inner hole with thread to connect a drive shaft (Higbee et al., 2013).

4.2.1 Geometry

The basis for impeller design is to properly define and process geometry. The Bladegen program was used for this purpose. The parameters are presented in Figure 4.3 and Table 4.1.

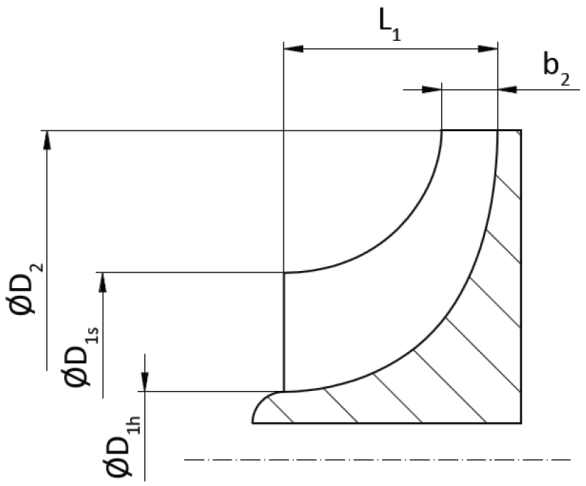

Figure 4.3: Basic parameters of the impeller.

Table 4.1: Basic parameters of the impeller.

Name	Symbol	Value	Units
Hub diameter	D_{1h}	30	mm
Shroud diameter	D_{1s}	83	mm
Impeller diameter	D_2	110	mm
Axial length	L_1	58	mm
Outlet impeller width	b_2	22	mm
Number of impeller blades	z	11	

Except the basic parameters, it is also necessary to determine the angles distribution along the blade. The impeller is divided into five layers which extend from the entrance to the end of wheel's edge (see Figure 4.5).

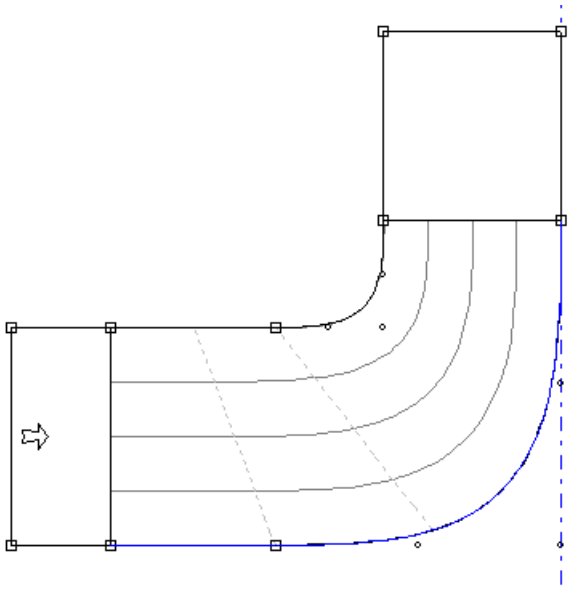

Figure 4.4: Distribution of the impeller to the layers.

The curvature of the blade is defined by β angle on each layer. Figure 4.5 shows that β is defined as the angle between the relative speed and the wheel axis.

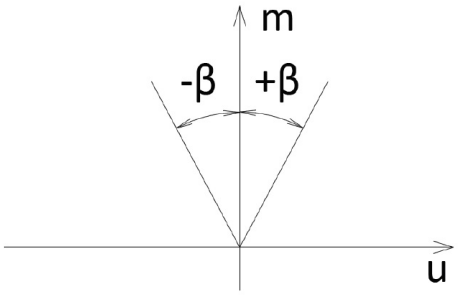

Figure 4.5: Definition of angular system in BladeGen.

Therefore the β angle is 0° on output. The β angle is set to 59° according to (Dixon, 2005) on impeller input. The remaining shape of the blade is formed as a smooth transition between angles on the input and output edge (see Figure 4.6). The horizontal axis is the distance (expressed in percentage) layer between the input and output edge on a layer.

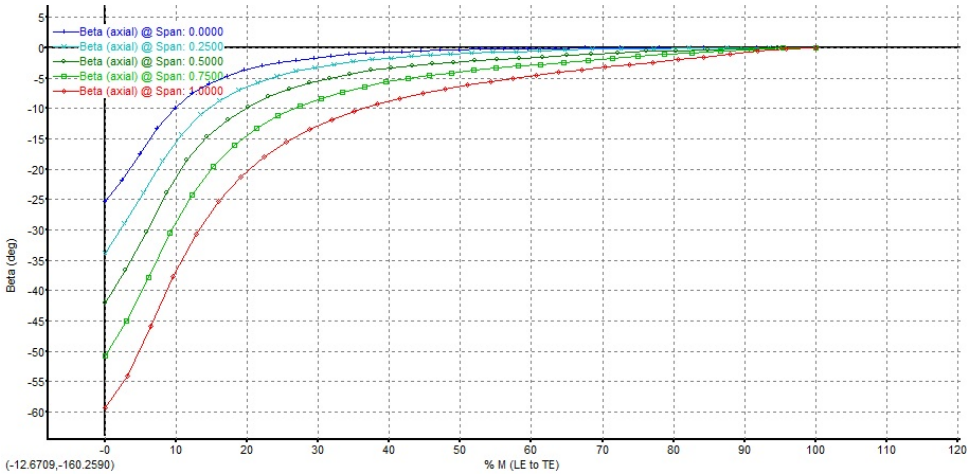

Figure 4.6: Distribution of the β angle on the impeller layers.

The last important parameter is the blades thickness. I have chosen a thickness of 1.7 mm due to the fact that the impeller was printed from plastic material. The resulting 3D model of the impeller of the centrifugal compressor with radial blades is depicted in Figure 4.7.

Figure 4.7: 3D model of the impeller of the centrifugal compressor.

4.2.2 Calculations

The following equations show the basic impeller calculations. Equation 4.1,Equation 4.2 offers the inlet flow area and outlet flow area computation. Determining the hydraulic diameter defines Equation 4.3.

$$A_1 = \pi \times \left(\left(\frac{D_{1s}}{2} \right)^2 - \left(\frac{D_{1h}}{2} \right)^2 \right) \tag{4.1}$$

$$A_2 = \pi \times D_2 \times b_2 \tag{4.2}$$

$$D_{hyd} = \frac{\pi \times \left(\frac{D_{1s} - D_{1h}}{2} \right) \times b_1}{z \times b_1 + \pi \times D_1} + \frac{\pi \times D_2 \times b_2}{z \times b_2 + \pi \times D_2} \tag{4.3}$$

4.2.3 Compressor structure

The centrifugal compressor consists of parts quoted in Table 4.2. Figure 4.8 and Figure 4.9 offers a depiction of individual components. The purpose was to craft as much components as possible using a 3D printer or CNC.

Table 4.2: Parts of the centrifugal compressor.

Name	Quantity	Obtained
Bolt M3x30 DIN 912	6	Purchased
Washer M3 DIN 125	6	Purchased
Nut M3 DIN 934	6	Purchased
Base	1	Crafted
Casing	1	Crafted
Engine MIG 400	1	Purchased
Foot	6	Crafted
Carrier	1	Crafted
Impeller	1	Crafted
Cover	1	Crafted

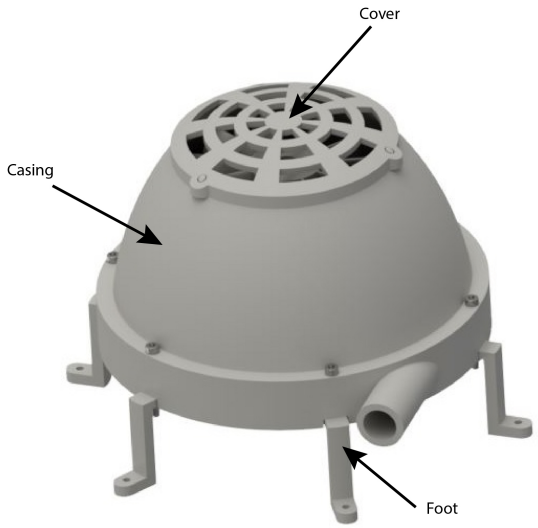

Figure 4.8: 3D model of the centrifugal compressor.

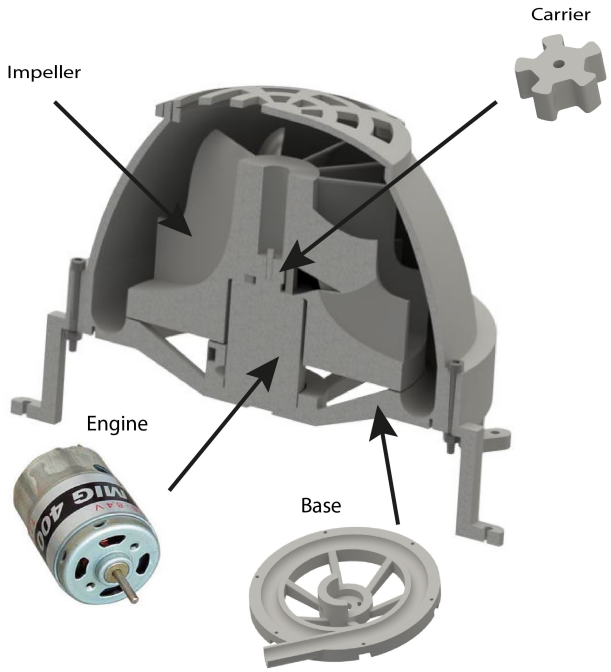

Figure 4.9: Sectional view of the centrifugal compressor.

4.2.4 High-Power Control

DC engine is controlled by the circuit shown in Figure 4.10. The main parts are Arduino and MOSFET which is a type of field-effect transistor (FET) with metal-oxide-semiconductor (MOS) structure. A resistor suits its purpose as a holder of low gate when the Arduino does not send a high signal. Significant component is a diode protecting MOSFET against damage. This diode is normally facing the wrong direction and does nothing. However, when that voltage spikes comes flowing the opposite direction, the diode allows it to flow back to the coil and not the transistor. Rectifier diode serves well in this case (see Platt, 2012).

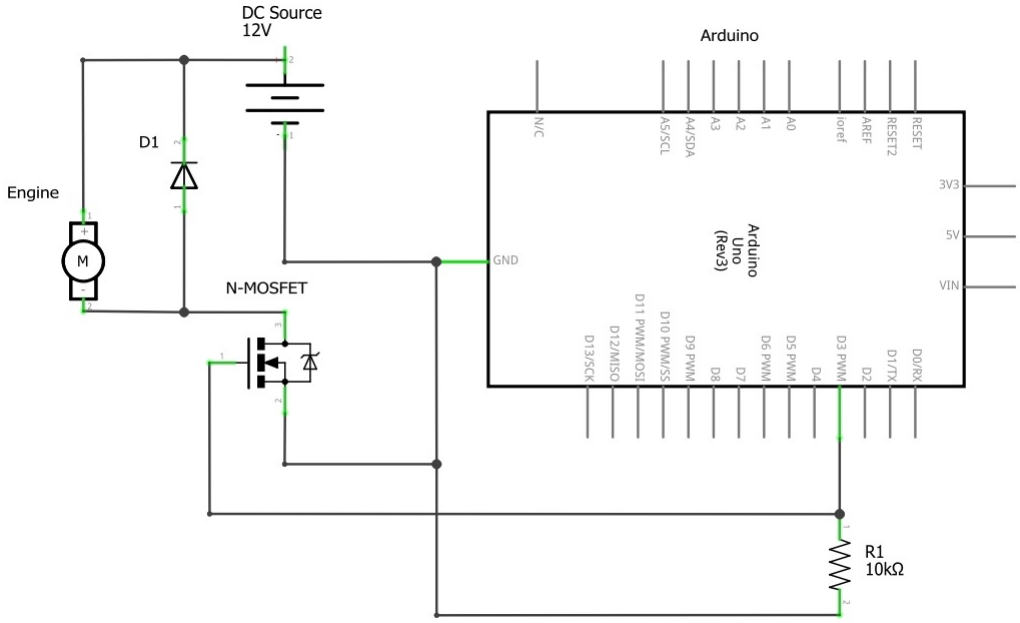

Figure 4.10: Circuit of controlling the DC motor.

Engine control is carried out by Pulse Width Modulation (PWM). It is a way for a digital device to output a pseudo-analogue signal. This technique allows digital device to output a pseudo-analogue signal. The Arduino is pulsing very quickly between 0 and 5 V so the average voltage is between 0 and 5 V. The transistor can only turn on or of in very short intervals. Therefore it is possible to fade lights or control the speed of a motor (Holmes and Lipo, 2003).

4.3 Air tank and pressure issue

Container of the original compressor which is designed for maximum of 10 bar serves as an air tank. The current pressure value is displayed using a manometer. The safety valve is mounted because of overpressure prevention. Pressure flowing into the Tesla turbine is controlled by two valves. First one is a solenoid valve automatically regulated by pressure sensor and switched via a relay. It has only only binary signal – open/closed so it is necessary to attach also a classic ball valve which is manually positioned and ensures required and constant output flow. Other solutions were also available. However, the solenoid valve is not controlled by PWM because of the high coil heating. It is desirable to add that also exists valves controlled by an analogue signal, but they are relatively expensive.

4.4 Tesla Turbine

Tesla turbine was chosen due to its relatively simple construction allowing self-help production. The turbine was invented and patented by Nikola Tesla at the beginning of the 20^{th} century. It works on the principle of compressed air, fluids or steam which is applied to the inlet and the turbine spins giving a mechanic rotational output. However, it can be designed as reversible device with no loss in efficiency. The Tesla turbine is blade-less therefore a disks attached to the shaft are used to create a torque (see Tesla, 1913).

Figure 4.11 provides 3D model of Tesla turbine. Components used for the construction are summarized in Table 4.3. The accent was on innovative design. HDD plates with vents milled on a CNC serves as a rotary discs. They are mounted on the aluminium bar to which the thread has been cut. It is connected to the shaft using washers and nuts. The shaft is a threaded rod which passes through the bar and ball bearings. The transparent tube fulfils the role of housing. Structural integrity is ensured by two perspex plates that are bolted together with four threaded rods, nuts and washers.

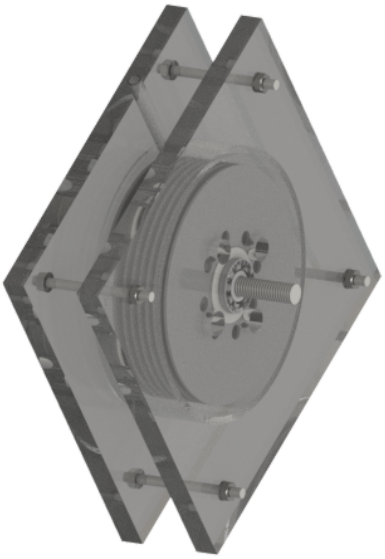

Figure 4.11: 3D view of the Tesla turbine.

Table 4.3: Components of the Tesla turbine.

Name	Quantity	Modified*
Perspex plate	2	Yes
HDD plate	7	Yes
Transparent tube ⌀110 mm	1	Yes
Aluminium bar ⌀25 mm	1	Yes
Shaft ⌀8 mm	1	No
Ball bearing	2	No
Nut M4 DIN 934	8	No
Nut M8 DIN 934	2	No
Washer M4 DIN 924	8	No
Penny washer M8 DIN 522	2	No
Threaded rod	4	No

*Requiring additional machining

4.5 Results

Parameters that were reached during model operation are summarized in Table 4.4. Input and output work of the model was calculated according to Equation 4.4. Subsequently, efficiency was calculated using Equation 4.5. It should be added that the

measurement was marked by a considerable degree of inaccuracy due to unstable power input and output. Therefore, the values are quite rough.

$$W = P \times t = V \times I \times t \tag{4.4}$$

$$\eta = \frac{W_{out}}{W_{in}} \tag{4.5}$$

Table 4.4: Operating values of energy storage model.

Operating pressure	Shaft RPM	W_{in}	W_{out}	Efficiency
6 bar	1,850	27 kJ	2.97 kJ	11 %

4.6 Conclusions

The main task of building a functional model of the energy storage technology was fulfilled in this chapter. At the beginning, the compressor was designed and printed using 3D technology. Production of the Tesla turbine using commonly available components followed. The design side of the model was completed by the acquisition of air tank, necessary fitting, sensors and a power generator. After that, valve control and PWM of the engine using Arduino was programmed. The model was completed at this time.

Testing under different operating conditions came up. At this point, it came out that although the manufactured centrifugal compressor was functional, it did not achieve sufficient overpressure. This was caused by used engine which was not powerful enough. For that reason, the piston compressor was purchased and used too. Other obstacles have not appeared and everything else has worked flawlessly. Finally, it is substantial to emphasize that the model served only as a CAES technology demonstration. This fact together with the use of home-made components caused that the model efficiency at 6 bar is 11 % (see Table 4.4).

Chapter 5

Calculations and Optimization via Python

The first part of the chapter aims to establish the isentropic efficiency and compression ratio of the radial compressor. This is accomplished by source code written in python which is described on the following pages. The goal is not to copy formulas that are programmed in python but suitably supplemented the code with the illustrations and comments. The second part of the chapter is dedicated to the optimization of geometry parameters for the best possible compression ratio of the centrifugal compressor. Thought out genetic algorithm serves to this purpose.

5.1 Introduction

5.1.1 Code structure

Source code consists of two main parts. Firstly, Calculation section which is written using the functional programming. Secondly, GUI programmed using object-oriented programming. Figure 5.1 provides a view of the user interface. Efficiency and compression ratio of the centrifugal compressor appears after entering values. There is also the option to render an inlet velocity triangle.

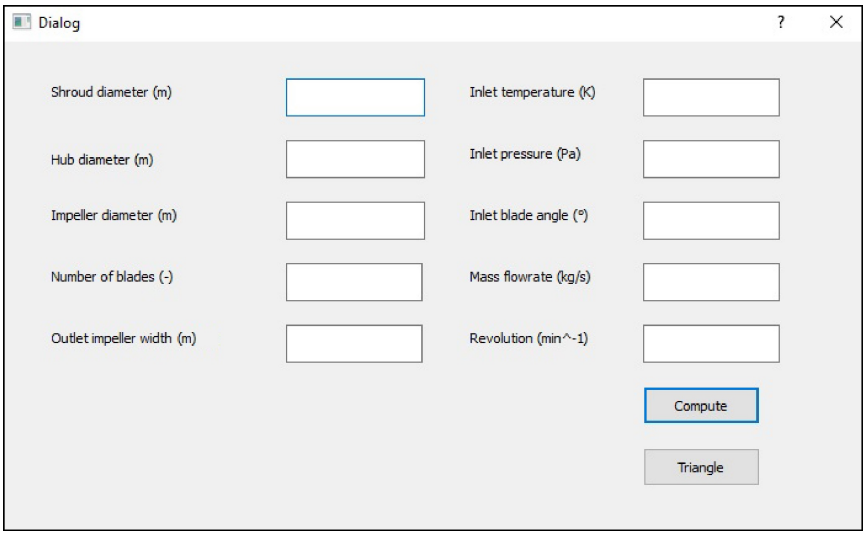

Figure 5.1: Graphical user interface.

5.1.2 Input parametres

The essential step is to define the operating parameters of centrifugal compressor (see Table 5.1).

Table 5.1: Operating conditions of the centrifugal compressor.

Name	Symbol	Value	Units
RPM of impeller	n	48,000	min^{-1}
Compressor mass flowrate	$\dot{m}$	1.1	$\mathrm{kg} \times \mathrm{s}^{-1}$
Ambient temperature	T_1	288	K
Atmospheric pressure	p_1	101,325	Pa

Computing software also requires a basic compressor geometry showed in Table 5.2.

Table 5.2: Geometry parameters of the centrifugal compressor.

Parameter	Value	Units
D_{1h}	0.0353	m
D_{1s}	0.106	m
D_2	0.174	m
b_2	0.0078	m
β_b	34.6	degree
z	16	–

All values presented in this subsection were determined on the basis of experience and data of various manufacturers.

5.2 Geometry computation

5.2.1 Impeller inlet

It is necessary to begin with computation of the parameters at the impeller inlet. This is executed with velocity triangle which is depicted in Figure 5.2.

If we consider the radial compressor, we can apply the following formula:

$$\alpha_1 = 90^\circ \rightarrow c_1 = c_{1m} \tag{5.1}$$

There is a mismatch between the fixed blade angle β_{1b} and the direction of the gas stream β_1 due to the to losses in the compressor. The angle of incidence is defined by

$$\beta_i = \beta_{1b} - \beta_1 \tag{5.2}$$

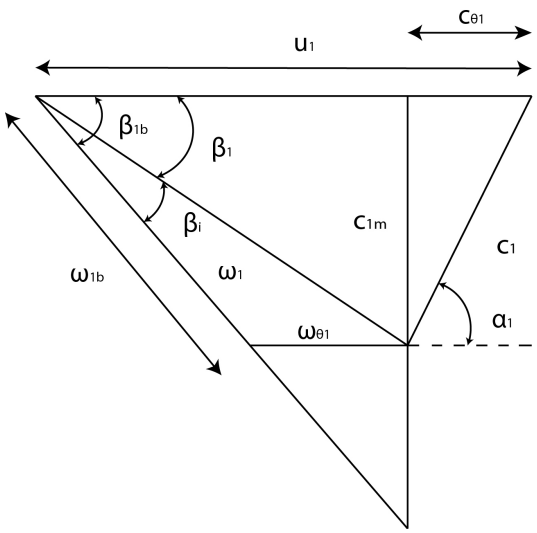

Figure 5.2: Inlet velocity triangle.

5.2.2 Impeller outlet

It is possible to consider for centrifugal compressor that the outlet radial component of absolute velocity is equal to total inlet velocity (Jiang et al., 2006).

$$c_{2r,b} = c_1 \tag{5.3}$$

Outlet relative velocity is equal to radial component of absolute velocity for radial vanes ($\beta_2 = 90°$) (Watson and Janota, 1982).

$$\omega_{2,b} = c_{2r,b} \tag{5.4}$$

The tangential component of the absolute velocity c_{2u} is reduced by slip. It is a phenomenon which is characteristic for a diversion of outlet relative velocity due to counter eddy in the channel between the vanes (see Figure 5.3) (Watson and Janota, 1982).

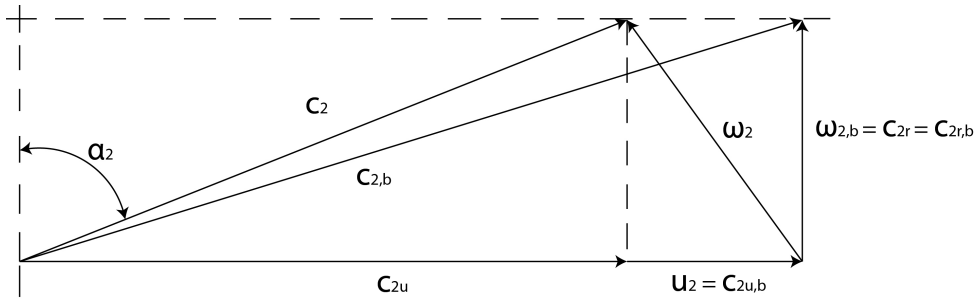

Figure 5.3: Outlet velocity triangle.

5.3 Impeller losses

Impeller losses significantly affect the efficiency of the centrifugal compressor. The following lines will be dedicated to the losses computation. It must be emphasized that there are many formulas for calculation of each type of loss and their results are sometimes relatively different.

5.3.1 Incidence loss

Incidence loss is caused by the direction of the gas flow diffusing from the blade angle (see Equation 5.2), which greatly affects the compressor performance characteristics at off-design conditions. Ferguson presented Equation 5.5 for incidence loss (Ferguson, 1963).

$$\Delta h_{inc} = \frac{1}{2} \times \left(u_1 - \frac{cotg\beta_{1b} \times \dot{m}}{\rho_{01} \times A_1} \right)^2 \tag{5.5}$$

5.3.2 Blade Loading Loss

Blade Loading Loss includes friction loss in boundary layers, secondary flow and swirling during flow separation. Equation 5.6 determinates the amount of lost energy (Coppage and Dallenbach, 1956).

$$\Delta h_{bld} = 0.05 \times D_f^2 \times u_2^2 \tag{5.6}$$

$$D_f = 1 - \frac{\omega_2}{\omega_{1s}} + \frac{\frac{0.75 \times \mu \times u_2^2}{u_2^2}}{\frac{\omega_{1s}}{\omega_2} \times \left(\left(\frac{z}{\pi} \right) \times \left(1 - \frac{D_{1s}}{D_2} \right) + \frac{2 \times D_{1s}}{D_2} \right)} \tag{5.7}$$

5.3.3 Skin friction loss

Skin friction losses are caused by shear forces in the boundary layer. The loss model express Equation 5.8 (Ferguson, 1963).

$$\Delta h_{sf} = \frac{C_h \times L_f \times \dot{m}^2}{2 \times D_{hyd} \times \rho_1^2 \times A_1^2 \times sin^2\beta_{1b}} \tag{5.8}$$

$$C_h = 4 \times 0.3164 \times Re^{-0.25} \tag{5.9}$$

5.3.4 Mixing loss

This type of loss is caused by unbalanced pressure velocity field closely behind the outlet of the impeller. The calculating of lost energy is described with the help of

Equation 5.10 (Howard, 1966).

$$\Delta h_{mix} = \frac{1}{1 + tan^2\alpha_2} \times \left(\frac{1 - \epsilon - b^*}{1 - \epsilon}\right) \times \frac{c_2^2}{2} \tag{5.10}$$

5.3.5 Recirculation Loss

Recirculation loss stems from the working fluid backflow into the impeller. The correlation is suggested by Equation 5.11 (Jansen, 1967).

$$\Delta h_{re} = 0.02 \times D_f^2 \times u_2^2 \times \sqrt{cotg\alpha_2} \tag{5.11}$$

5.3.6 Results

Results of the centrifugal compressor computation defined in the Table 5.1 and in Table 5.2 are summarized in Table 5.3. Despite the considered losses, calculated efficiency is quite high and there is not much room for improvement. On the other hand, it is possible to increase the compression ratio with the help of tiny changes in the impeller geometry (see Subsection 5.4.2).

Table 5.3: The resulting compression ratio and efficiency of the centrifugal compressor.

Name	Value	Unit
Compression ratio	4.2	–
Efficiency	0.87	–

5.4 Genetics Algorithm

5.4.1 Introduction

Genetic algorithms are considered as the most popular evolutionary computation techniques and were first introduced by John Holland (Holland, 1975). GAs are inspired by the concept of Darwin's theory of evolution where the population is evolved by means of natural selection and survival of the fittest over many generations. This concept has been translated into computer algorithms so the terminology was copied from biology. The process starts by creating initial population formed by a collection of individuals which symbolize possible solutions to a solving problem. The individual consists of a chromosome which is a sequence of genes. Genes can be understood as a parameter set describing a possible solution. There exist different ways of representing individual genes such as bits and numbers. The chromosomes are then tested for their performance called fitness with the quality function. The function is an abstract fitness measure which selects suitable chromosomes of the initial population to seed the next generation by applying crossover and mutation to them (Simon, 2013). Executing the crossover and mutation to parents results in a set of new candidates named offspring which compete (based on selection technique) with the old ones for the place in the next generation. There is a wide variety of GA selection techniques such as roulette wheel selection, rank selection, and tournament selection (Mitchell, 1998). Figure 5.4 represents the method proposed in this section which uses a combination of rank selection, elitism, and elimination of the weakest individuals.

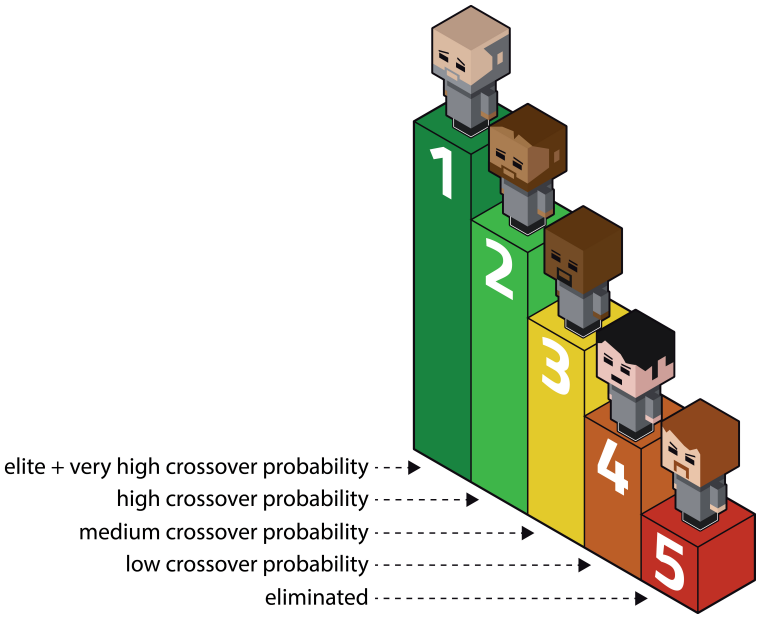

Figure 5.4: Combination of rank selection, elitism, and elimination of the weakest individuals.

The crossover procedure handles exchange of the genetic material between two chromosomes and creates two new offspring (see Figure 5.5). After that, mutation operator is applied for a purpose of increasing genetic diversity of the population. Finally, a new generation is created and the whole process is iterated until a sufficient solution is found (Sivanandam and Deepa, 2007).

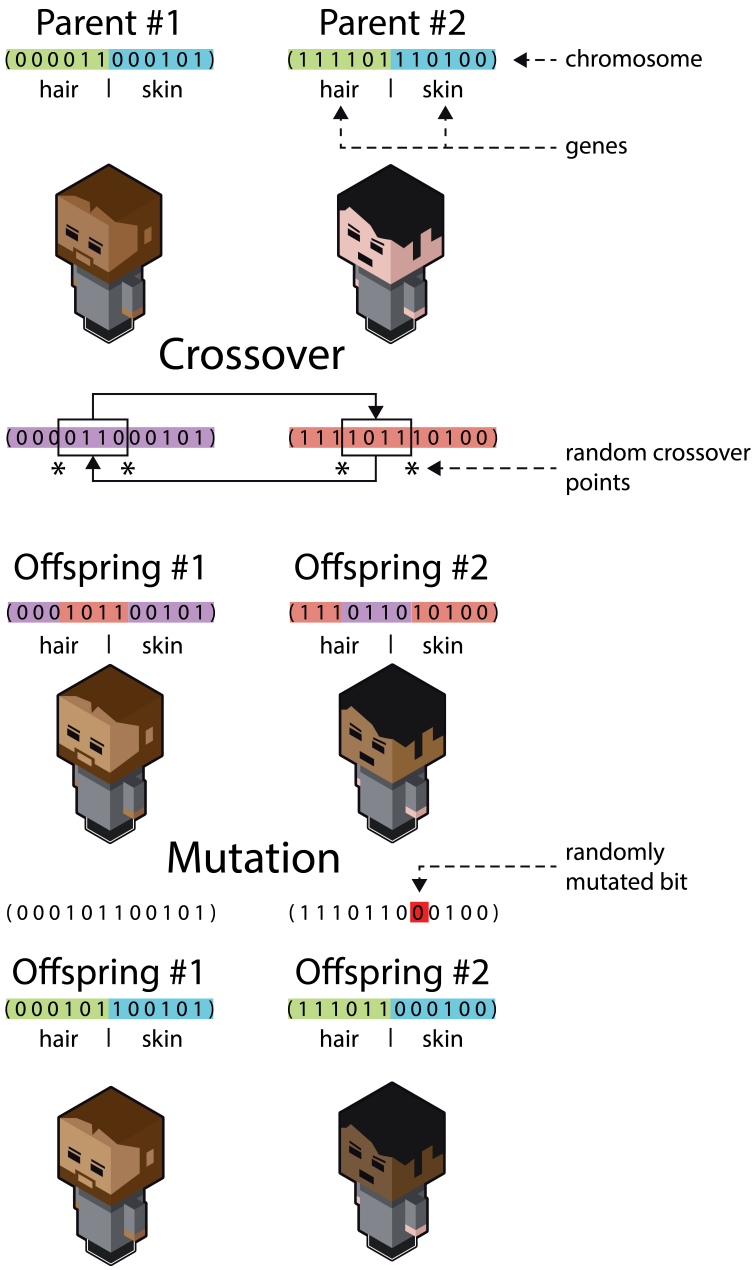

Figure 5.5: Overview of GA operators.

The whole process of genetic algorithm is encapsulated using pseudo code in Algorithm 5.1.

Algorithm 5.1 General genetic algorithm.

```
1: ENTER(inPar);                                   ▷ Enter input parameters
2: i ← 0;
3: P(0) ← GENINITPOP(inPar);                       ▷ Generate initial population
4: EVALPOP(P(0));                                  ▷ Evaluate each individual
5: while not in the termination condition do
6:     P_p(i) ← SELECT(P(i));                      ▷ Select parents
7:     P_o(i) ← CROSSOVER(P_p(i));                 ▷ Crossover parents
8:     MUTATE(P_o(i));                             ▷ Mutate offsprings
9:     P(i + 1) ← REPLACE(P_o(i), P(i));           ▷ Replace old population
10:    EVALPOP(P(i + 1));                          ▷ Evaluate each individual
11:    i ← i + 1;
12: end while
```

5.4.2 Compress ratio optimization

The GA code uses input parameters that are summarized in Table 5.1 and also in Table 5.3. The aim of the calculation was to achieve the highest compression ratio with respect to defined intervals of impeller geometry. Table 5.4 shows overview of the optimization computation.

Table 5.4: Optimization overview.

Parameter	Value	Interval	Optimizated parameter	Units
D_{1h}	0.0353	[0.02, 0.06]	0.034	m
D_{1s}	0.106	[0.086, 0.126]	0.113	m
D_2	0.174	[0.154, 0.194]	0.194	m
b_2	0.0078	[0.0028, 0.0108]	0.0085	m
β_b	34.6	[30, 60]	31.5	degree
z	16	[15, 20]	20	–
η	0.87	–	0.91	–
Π	4.2	–	5.9	–

It is necessary to define design restrictions for proper optimization. Equation 5.12 and Equation 5.13 defining recommended relationships with respect to strength of the impeller.

$$D_{1s} = (0,45 \sim 0,6) \times D_2 \tag{5.12}$$

$$D_{1h} = (0,3 \sim 0,6) \times D_{1s} \tag{5.13}$$

It is also necessary to eliminate the shock wave (see Equation 5.14) forming before the impeller inlet.

$$Ma_{1,rel} < 1 \tag{5.14}$$

Finally, the slip coefficient check is done. Selected μ must not differ from calculated $\mu^{'}$ by more than 2 %. Calculation offer Equation 5.15, Equation 5.16 and Equation 5.17.

$$\mu^{'} = \frac{1}{1 + \left(\frac{2\times\pi}{3\times z}\right) \times \frac{1}{1-\left(\frac{D_{mid}}{D_2}\right)^2}} \tag{5.15}$$

$$\mu = (0,86 \sim 0,92) \tag{5.16}$$

$$\left(\frac{\mu^{'} - \mu}{\mu^{'}}\right) \times 100 < 2 \tag{5.17}$$

Figure 5.6 offers development of best individual in the population during generations for six independent calculations. The improvement of individual is noticeable from 1 to 6 generation. The first 15 generations are shown for illustration because the continuing curve trend is almost constant. However, the calculation was performed for 5000 generations in order to maximize the accuracy.

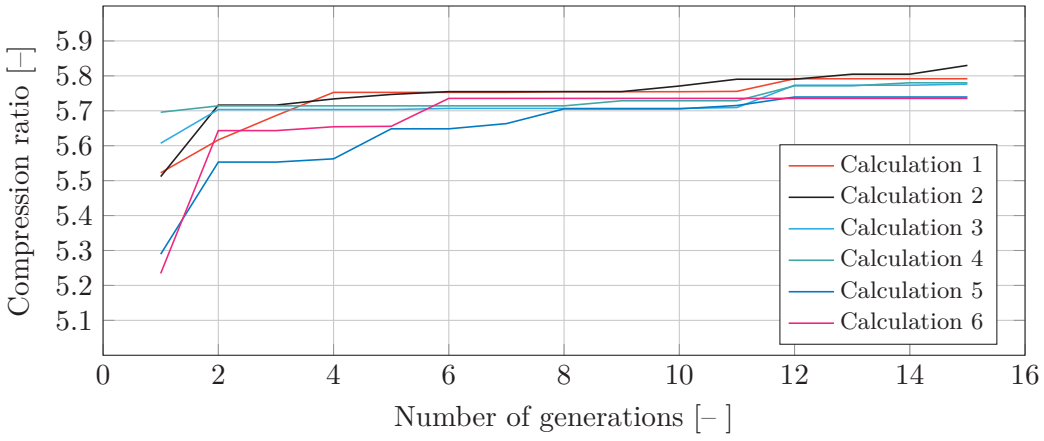

Figure 5.6: The development of best individual in the process of generations

5.5 Conclusion

Software computing efficiency and compression ratio of the centrifugal compressor was developed in this chapter. Subsequently, the graphical user interface was programmed for better controllability. Then I have asked myself: *"Is it possible to improve compression ratio of defined compressor?"*. Genetic algorithm was programmed to find the answer. Achieved result speaks for itself – improvement of the compression ratio by almost 30 %. Finally, it should be noted that the calculation was limited by strength conditions and dimension intervals (see Table 5.4).

Chapter 6

Conclusions

The following chapter summarizes bachelor thesis and points out the most important findings. It also offers suggestions for possible future work.

6.1 Summary

The first part of the thesis deals with the issue of Carbon Capture and Storage. As it turned out, this technology is very costly and it is logical to ask whether it can be successfully implemented in the foreseeable future. The political situation in the field of power engineering and ecology will indicate a lot. The essential fact is that money for development of the CCS technology was earned primarily from oil companies. The reason is simple – it is possible to extract more oil using injecting carbon dioxide into storage with oil. However, in the present condition when oil is very cheap, this method is economically very disadvantageous.

It is currently being considered to implement CCS technology into the energy storage technology chain. There is obvious a great potential which depends on development and expansion of renewable energy sources. RES will not be competitive without the efficient accumulation of electricity and this technology offers one of the possible ways.

The practical part of my thesis started by building a model of CAES technology. My motivation was to create something tangible and to experience all the pitfalls, problems that are related to it. As a student of the Faculty of Mechanical Engineering, I used the knowledge acquired by my previous study and also self-study. I have found

out that building a functioning device is not easy at all, but the result was definitely worth it. The model worked as I have expected and was able to produce electricity. I am convinced that this experience will help me in my future career, for example, in the construction of experimental devices verifying the theoretical calculations.

I have engaged in programming in the second section of my practical part. The first assignment was to program SW for calculating the efficiency and compression ratio of the centrifugal compressor. Surprisingly, the creation of user-friendly GUI was the biggest challenge there. Afterwards, I have successfully tested the software outputs to verify them. Since I was tempted by the concept of genetic algorithm, I have decided to program it and try it out. A compression ratio of radial compressor served as a test experiment. The task was to maximize this parameter using slight changes in the geometry. The result was an increase of the compression ratio by almost 30 %. So it can be stated that the genetic algorithm fulfilled its function and was programmed correctly.

6.2 Contributions of bachelor thesis

The main contributions of this thesis are as follows (more is provided at the end of each respective chapter):

In Chapter 2:

Description of Carbon Capture and Storage technology, including overview of the topic, the economic costs and existing projects.

In Chapter 3:

Research on the Compressed Air Energy Storage offering necessary information and existing projects.

In Chapter 4:

Construction of the functional model storing compressed air and generating electric energy subsequently.

In Chapter 5:

Calculation of centrifugal compressor isentropic efficiency, compression ratio using python and optimization with the help of genetic algorithm.

6.3 Future work

It is suggested to explore the following:

- Use CO_2 instead of compressed air as the fluid in the model described in Chapter 4.
- Usage of the program described in Chapter 5 for compressor characteristics programming.
- Utilization of the genetic algorithm in the future projects.

6.4 Afterword

I started to work on the thesis nearly a year in advance – in July 2016. The reason and my motivation during research as well can be expressed with the quote of American speaker Jim Rohn: *"Formal education will make you a living. Self–education will make you a fortune."* Fortune is in my point of view understood in two ways and these are material and especially mental. So I frankly believe that hard work and effort to gain a lot of new knowledge will lead to confirmation of the Rohn's thought.

Bibliography

Adams, E. and Caldeira, K. (2008). Ocean storage of CO_2. *Elements*, 4(5):319–324.

Akai, M., Nishio, N., Iijima, M., Ozaki, M., Minamiura, J., and Tanaka, T. (2004). Performance and economic evaluation of CO_2 capture and sequestration technologies. In *Proceedings of the Seventh International Conference on Greenhouse Gas Control Technologies*. Elsevier.

Al-Fattah, S. M., Barghouty, M., and Dabbousi, B. (2011). *Carbon Capture and Storage: Technologies, Policies, Economics, and Implementation Strategies*. CRC Press.

Alaceas (2015). ALACAES an airlight energy company. `https://alacaes.com/`.

Alendal, G. and Drange, H. (2001). Two-phase, near-field modeling of purposefully released CO_2 in the ocean. *Journal of geophysical research*, 106(C1):1085–1096.

Anheden, M., Burchhardt, U., Ecke, H., Faber, R., Jidinger, O., Giering, R., Kass, H., Lysk, S., Ramström, E., and Yan, J. (2011). Overview of operational experience and results from test activities in vattenfall's 30 MW_{th} oxyfuel pilot plant in schwarze pumpe. *Energy Procedia*, 4:941–950.

ARS (2010 (accessed July 4, 2016)). *Map of internmational CO_2 pipeline between Beulah, ND, USA and Weyburn, SK, CAN.* `http://neori.org/wp-content/uploads/2012/02/HowCO2EORWorks_Graphic2.png`.

Aspelund, A. and Jordal, K. (2007). Gas conditioning—the interface between CO_2 capture and transport. *International Journal of Greenhouse Gas Control*, 1(3):343–354.

Aspelund, A., Molnvik, M., and De Koeijer, G. (2006). Ship transport of CO_2: Technical solutions and analysis of costs, energy utilization, exergy efficiency and CO_2 emissions. *Chemical Engineering Research and Design*, 84(9):847–855.

Baxter, L. (2015). Cryogenic Carbon Capture^{TM} as a Holistic Approach to a Low-Emissions Energy System. `http://cornerstonemag.net/tag/high-efficiency-coal/`.

Bermúdez, J., Arenillas, A., Luque, R., and Menéndez, J. (2013). An overview of novel technologies to valorise coke oven gas surplus. *Fuel processing technology*, 110:150–159.

Birkholzer, J., Zhou, Q., and Tsang, C.-F. (2009). Large-scale impact of CO_2 storage in deep saline aquifers: A sensitivity study on pressure response in stratified systems. *International Journal of Greenhouse Gas Control*, 3(2):181–194.

Birol, F., Cozzi, L., Morgan, R., and A., B. (2009). *World Energy Outlook*. Organization for Economic Cooperation & Devel.

Bock, B., Rhudy, R., Herzog, H., Klett, M., Davidson, J., De la Torre, D., and Simbeck, D. (2003). Economic evaluation of CO_2 storage and sink options. Technical report, Department of Energy, Pittsbrough Energy Technology Center.

Brandvoll, O. and Bolland, O. (2002). Inherent CO_2 capture using chemical looping combustion in a natural gas fired power cycle. In *ASME Turbo Expo 2002: Power for Land, Sea, and Air*, pages 493–499. American Society of Mechanical Engineers.

Brunetti, A., Scura, F., Barbieri, G., and Drioli, E. (2010). Membrane technologies for CO_2 separation. *Journal of Membrane Science*, 359(1):115–125.

Budt, M., Wolf, D., Span, R., and Yan, J. (2016). A review on compressed air energy storage: Basic principles, past milestones and recent developments. *Applied Energy*, 170:250–268.

Buhre, B., Elliott, L., Sheng, C., Gupta, R., and Wall, T. (2005). Oxy-fuel combustion technology for coal-fired power generation. *Progress in energy and combustion science*, 31(4):283–307.

Bullough, C., Gatzen, C., Jakiel, C., Koller, M., Nowi, A., and Zunft, S. (2004). Advanced adiabatic compressed air energy storage for the integration of wind energy. In *Proceedings of the European Wind Energy Conference, EWEC*, volume 22, page 25.

Castellani, B., Filipponi, M., Nicolini, A., Cotana, F., and Rossi, F. (2013). Carbon dioxide capture using gas hydrate technology. *Journal of Energy and Power Engineering*, 7(5):883.

Cheng-Hsiu, Y. (2012). A review of CO_2 capture by absorption and adsorption. *Aerosol Air Qual. Res*, 12(5):745–769.

Chino, K. and Araki, H. (2000). Evaluation of energy storage method using liquid air. *Heat Transfer—Asian Research*, 29(5):347–357.

Clark, J., Bonura, D., and Van Voorhees, R. (2005). An overview of injection well history in the united states of america. *Developments in Water Science*, 52:3–12.

Collins, S. (1993). Commercial options for energy storage multiply. *Power;(United States)*, 137(1).

Coppage, J. and Dallenbach, F. (1956). Study of supersonic radial compressors for refrigeration and pressurization systems. Technical report, DTIC Document.

Crotogino, F., Mohmeyer, K., and Scharf, R. (2001). Huntorf caes: More than 20 years of successful operation. *Orlando, Florida, USA*.

Dahowski, R. and Dooley, J. (2005). *Building the Cost Curves for CO_2 Storage: North America*. IEA Greenhouse Gas R & D Programmee.

D'Alessandro, D., Smit, B., and Long, J. (2010). Carbon dioxide capture: Prospects for new materials. *Angewandte Chemie International Edition*, 49(35):6058–6082.

DGC (2008 (accessed July 4, 2016)). *Map of internmational CO_2 pipeline between Beulah, ND, USA and Weyburn, SK, CAN.* `https://hub.globalccsinstitute.com/sites/default/files/publications/books/151303/images/fig07.jpg`.

Dixon, S. L. (2005). *Fluid Mechanics and Thermodynamics of Turbomachinery*. Elsevier Science.

Eckroad, S. and Gyuk, I. (2003). Epri-doe handbook of energy storage for transmission & distribution applications. *Electric Power Research Institute, Inc.*

Ferguson, T. (1963). *The centrifugal compressor stage*. Butterworths.

Gale, J. and Davidson, J. (2004). Transmission of CO_2 — safety and economic considerations. *Energy*, 29(9):1319–1328.

Garvey, S. and Pimm, A. (2016). Compressed air energy storage. In Letcher, T., editor, *Storing Energy: with Special Reference to Renewable Energy Sources*, chapter 5, pages 87–111. Elsevier.

Godec, M., Kuuskraa, V., Van Leuwen, T., Melzer, L., and Wildgust, N. (2011). CO_2 storage in depleted oil fields: The worldwide potential for carbon dioxide enhanced oil recovery. *Energy Procedia*, 4:2162–2169.

Haszeldine, R. (2009). Carbon capture and storage: How green can black be? *Science*, 325(5948):1647–1652.

Helsingen, E. (2015). Adiabatic compressed air energy storage. Master's thesis, Norwegian University of Science and Technology, Trondheim, Norway.

Higbee, R. W., Giacomelli, J. J., and Wyczalkowski, W. R. (2013). Advanced impeller design: Anti-ragging impeller, ari2. *Chemical Engineering Research and Design*, 91(11):2190–2197.

Hoffeins, H. and Mohmeyer, K. (1986). Operating experience with the huntorf air-storage gas turbine power station. *Brown Boveri Review*, 73(6):297–305.

Holland, J. H. (1975). *Adaption in natural and artificial systems*. Ann Arbor MI: The University of Michigan Press.

Holmes, D. G. and Lipo, T. A. (2003). *Pulse width modulation for power converters: principles and practice*, volume 18. John Wiley & Sons.

Howard, J. (1966). Discussion:"losses in vaneless diffusers of centrifugal compressors and pumps: Analysis, experiment, and design"(johnston, jp, and dean, jr., rc, 1966, asme j. eng. power, 88, pp. 49–60). *Journal of Engineering for Power*, 88(1):60–61.

Ibrahim, H., Belmokhtar, K., and Ghandour, M. (2015). Investigation of usage of compressed air energy storage for power generation system improving-application in a microgrid integrating wind energy. *Energy Procedia*, 73:305–316.

IPCC (2014). *Climate Change 2014–Impacts, Adaptation and Vulnerability: Regional Aspects*. Cambridge University Press.

Jansen, D., Gazzani, M., Manzolini, G., van Dijk, E., and Carbo, M. (2015). Pre-combustion CO_2 capture. *International Journal of Greenhouse Gas Control*, 40:167–187.

Jansen, W. (1967). A method for calculating the flow in a centrifugal impeller when entropy gradients are present. In *Royal Society conference on internal aerodynamics (turbomachinery)*, pages 133–146.

Jiang, W., Khan, J., and Dougal, R. A. (2006). Dynamic centrifugal compressor model for system simulation. *Journal of power sources*, 158(2):1333–1343.

Kalhammer, F. R. and Schneider, T. R. (1976). Energy storage. *Annual Review of Energy*, 1(1):311–343.

Khan, C., Amin, R., and Madden, G. (2013). Carbon dioxide injection for enhanced gas recovery and storage (reservoir simulation). *Egyptian Journal of Petroleum*, 22(2):225–240.

Kim, Y., Lee, J., Kim, S., and Favrat, D. (2012). Potential and evolution of compressed air energy storage: energy and exergy analyses. *Entropy*, 14(8):1501–1521.

Lemofouet-Gatsi, S. (2006). *Investigation and optimisation of hybrid electricity storage systems based on compressed air and supercapacitors*. PhD thesis, Citeseer.

Leung, D., Caramanna, G., and Maroto-Valer, M. (2014). An overview of current status of carbon dioxide capture and storage technologies. *Renewable and Sustainable Energy Reviews*, 39:426–443.

Li, J., Ma, Y., McCarthy, M., Sculley, J., Yu, J., Jeong, H., Balbuena, P., and Zhou, H. (2011). Carbon dioxide capture-related gas adsorption and separation in metal-organic frameworks. *Coordination Chemistry Reviews*, 255(15):1791–1823.

Li, Z., Dong, M., Li, S., and Huang, S. (2006). CO_2 sequestration in depleted oil and gas reservoirs—caprock characterization and storage capacity. *Energy Conversion and Management*, 47(11):1372–1382.

Loose, V. W. (2011). Quantifying the value of hydropower in the electric grid: Role of hydropower in existing markets. *Sandia National Laboratories*.

Lund, H. and Salgi, G. (2009). The role of compressed air energy storage (caes) in future sustainable energy systems. *Energy conversion and management*, 50(5):1172–1179.

Luo, X., Wang, J., Dooner, M., and Clarke, J. (2015). Overview of current development in electrical energy storage technologies and the application potential in power system operation. *Applied Energy*, 137:511–536.

Maroto-Valer, M. (2010a). *Developments and Innovation in Carbon Dioxide (CO_2) Capture and Storage Technology Volume 1: Carbon dioxide (CO_2) capture, transport and industrial applications*. Woodhead Publishing.

Maroto-Valer, M. (2010b). *Developments and Innovation in Carbon Dioxide (CO_2) Capture and Storage Technology Volume 2: Carbon dioxide (CO_2) storage and utilisation*. Woodhead Publishing.

Mason, J. E. and Archer, C. L. (2012). Baseload electricity from wind via compressed air energy storage (caes). *Renewable and Sustainable Energy Reviews*, 16(2):1099–1109.

Masoudian, M. (2016). Multiphysics of carbon dioxide sequestration in coalbeds: A review with a focus on geomechanical characteristics of coal. *Journal of Rock Mechanics and Geotechnical Engineering*, 8(1):93–112.

McCoy, S. T. and Rubin, E. S. (2008). An engineering-economic model of pipeline transport of CO_2 with application to carbon capture and storage. *International journal of greenhouse gas control*, 2(2):219–229.

Metz, B., Davidson, O., Coninck, H., Loos, M., and Meyer, L. (2005). *Carbon Dioxide Capture and Storage*. Cambridge University Press.

Mitchell, M. (1998). *An introduction to genetic algorithms*. MIT press.

Monne, J. and Prinet, C. (2013). Lacq-rousse industrial ccs reference project: description and operational feedback after two and half years of operation. *Energy Procedia*, 37:6444–6457.

Morgan, R., Nelmes, S., Gibson, E., and Brett, G. (2015). Liquid air energy storage–analysis and first results from a pilot scale demonstration plant. *Applied Energy*, 137:845–853.

Moritis, G. (2003). CO_2 sequestration adds new dimension to oil, gas production. *Oil & Gas Journal*, 101:71–83.

Nakhamkin, M., Andersson, L., Swensen, E., Howard, J., Meyer, R., Schainker, R., Pollak, R., and Mehta, B. (1992). Aec 110 mw caes plant: status of project. *Journal of engineering for gas turbines and power*, 114(4):695–700.

Neele, F., Haugen, H., and Skagestad, R. (2014). Ship transport of CO_2 – breaking the co2-eor deadlock. *Energy Procedia*, 63:2638–2644.

Oelkers, E., Gislason, S., and Matter, J. (2008). Mineral carbonation of CO_2. *Elements*, 4(5):333–337.

Olajire, A. (2013). A review of mineral carbonation technology in sequestration of CO_2. *Journal of Petroleum Science and Engineering*, 109:364–392.

Oldenburg, C., Pruess, K., and Benson, S. (2001). Process modeling of CO_2 injection into natural gas reservoirs for carbon sequestration and enhanced gas recovery. *Energy & Fuels*, 15(2):293–298.

Oldenburg, C., Pruess, K., and Benson, S. (2004). Economic feasibility of carbon sequestration with enhanced gas recovery (csegr). *Energy*, 29(9):1413–1422.

Ozaki, M., Minamiura, J., Kitajima, Y., Mizokami, S., Takeuchi, K., and Hatakenaka, K. (2001). CO_2 ocean sequestration by moving ships. *Journal of Marine Science and Technology*, 6(2):51–58.

Platt, C. (2012). *Encyclopedia of Electronic Components Volume 1: Resistors, Capacitors, Inductors, Switches, Encoders, Relays, Transistors*, volume 1. " O'Reilly Media, Inc.".

Pollak, R. (1994). History of first us compressed-air energy storage (caes) plant (110 mw 26h) volume 2: Construction. *Electric Power Research Institute (EPRI)*.

Power, R. (2012). Adele–adiabatic compressed-air energy storage for electricity supply.

Preston, C., Whittaker, S., Rostron, B., Chalaturnyk, R., White, D., Hawkes, C., Johnson, J., Wilkinson, A., and Sacuta, N. (2009). Iea ghg weyburn-midale CO_2 monitoring and storage project–moving forward with the final phase. *Energy Procedia*, 1(1):1743–1750.

Radgen, P. (2008). 30 years compressed air energy storage plant huntorf—experiences and outlook. In *Proceedings of the 3rd International Renewable Energy Storage Conference, Berlin, Germany*, pages 24–25.

Rao, A. and Rubin, E. (2002). A technical, economic and environmental assessment of amine-based co2 capture technology for power plant greenhouse gas control. *Environmental Science & Technology*, 36:4467–4475.

Riding, J. (2006). The iea weyburn CO_2 monitoring and storage project. In *Advances in the Geological Storage of Carbon Dioxide*, pages 221–230. Springer.

Ringrose, P., Mathieson, A., Wright, I., Selama, F., Hansen, O., Bissell, R., Saoula, N., and Midgley, J. (2013). The in salah CO_2 storage project: lessons learned and knowledge transfer. *Energy Procedia*, 37:6226–6236.

Rogers, G. and Mayhew, Y. (1980). *Thermodynamic and Transport Properties of Fluids*. Blackwell Publishing.

Rubin, E., Davidson, J., and Herzog, H. (2015). The cost of CO_2 capture and storage. *Greenhouse Gas Control*, 40:378–400.

Rubin, E., Rao, A., and Chen, C. (2003). Understanding the cost of CO_2 capture and storage for fossil fuel power plants. Technical report, Department of Engineering and Public Policy, Carnegie Mellon University, Pittsbrough.

Rybalchenko, A., Pimenov, M., Kurochkin, V., Kamnev, E., Korotkevich, V., Zubkov, A., and Khafizov, R. (2005). Deep injection disposal of liquid radioactive waste in russia, 1963–2002: Results and consequences. *Developments in Water Science*, 52:13–19.

Sandén, B. (2014). Systems perspectives on renewable power 2014.

Sheng, J. (2013). *Enhanced Oil Recovery Field Case Studies*. Gulf Professional Publishing.

Simon, D. (2013). *Evolutionary optimization algorithms*. John Wiley & Sons.

Sivanandam, S. N. and Deepa, S. N. (2007). *Introduction to genetic algorithms*. Springer Science & Business Media.

Tesla, N. (1913). Turbine. US Patent 1,061,206.

Torp, T. and Gale, J. (2004). Demonstrating storage of CO_2 in geological reservoirs: the sleipner and sacs projects. *Energy*, 29(9):1361–1369.

Vattenfall (2008 (accessed July 4, 2016)). *Coal carbon capture and storage site at Schwarze Pumpe, Germany*. `http://news.bbc.co.uk/nol/shared/bsp/hi/image_maps/08/1219000000/1219932016/img/ccs_plant_466.gif`.

Venkataramani, G., Parankusam, P., Ramalingam, V., and Wang, J. (2016). A review on compressed air energy storage–a pathway for smart grid and polygeneration. *Renewable and Sustainable Energy Reviews*, 62:895–907.

Watson, N. and Janota, M. S. (1982). *Turbocharging: The internal combustion engine*. Macmillan.

White, C., Smith, D., Jones, K., Goodman, A., Jikich, S., LaCount, R., DuBose, S., Ozdemir, E., Morsi, B., and Schroeder, K. (2005). Sequestration of carbon dioxide in coal with enhanced coalbed methane recoverys a review. *Energy & Fuels*, 19(3):659–724.

White, C., Strazisar, B., Granite, E., Hoffman, J., and Pennline, H. (2003). Separation and capture of CO_2 from large stationary sources and sequestration in geological formations—coalbeds and deep saline aquifers. *Journal of the Air & Waste Management Association*, 53(6):645–715.

Wilcox, J. (2012). *Carbon Capture*. Springer Science & Business Media.

Wolf, D. (2011). *Methods for Design and Application of Adiabatic Compressed Air Energy: Storage Based on Dynamic Modeling*. UMSICHT-Schriftenreihe. Laufen.

Wolf, D. and Budt, M. (2014). Lta-caes–a low-temperature approach to adiabatic compressed air energy storage. *Applied Energy*, 125:158–164.

Wong, S. (2012 (accessed July 5, 2016)). *A spiral wound module showing the separation of carbon dioxide from other gases*. `https://hub.globalccsinstitute.com/sites/default/files/publications/books/189778/images/fig26.jpgf`.

Wong, S. and Bioletti, R. (2002). Carbon dioxide separation technologies. *Alberta Research Council*.

ZEP (2011). *The costs of CO_2 storage: post-demonstration CCS in the EU*. European Technology Platform for Zero Emission Fossil Fuel Power Plants.

List of Appendices

Appendix A

Assembled supportive devices

A.1 Shapeoko 2

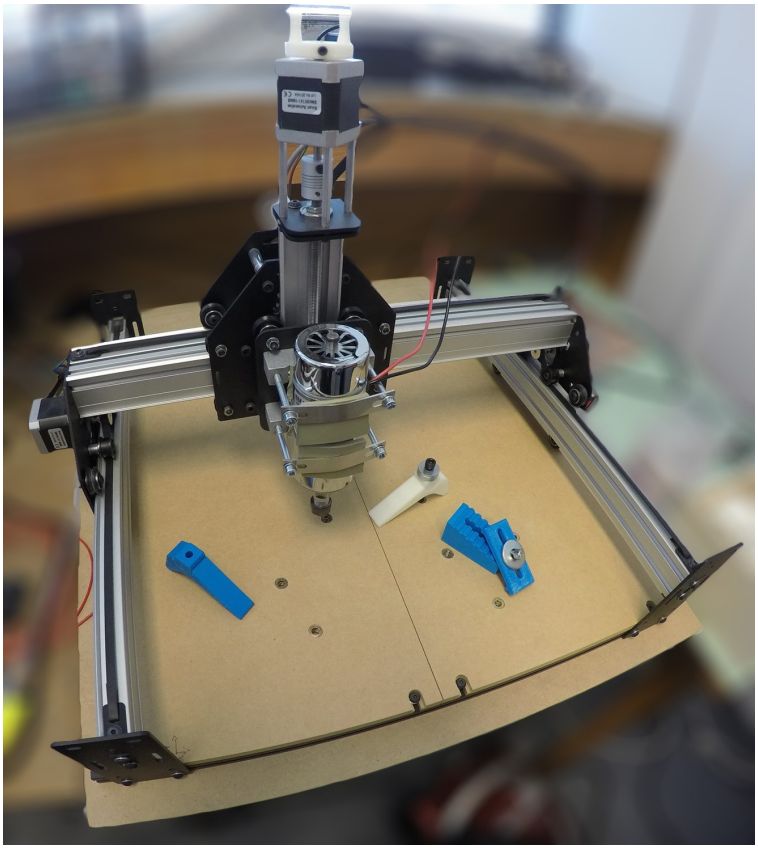

Figure A.1: Open-source CNC mill Shapeoko 2.

A.2 Prusa i3

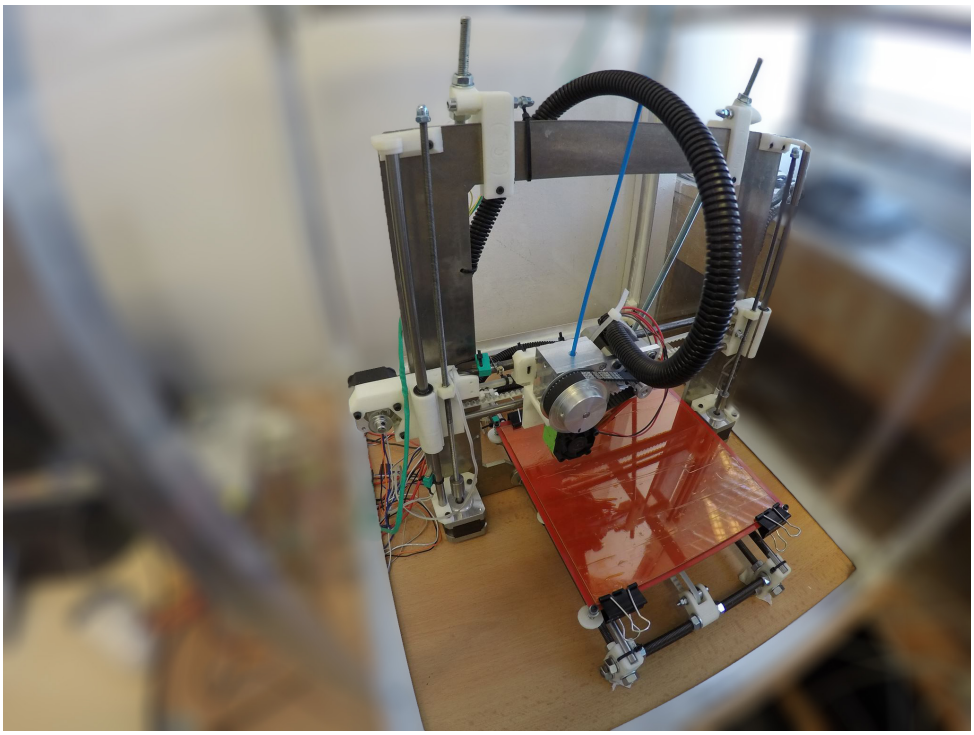

Figure A.2: Open-source 3D printer Prusa i3.